

See discussions, stats, and author profiles for this publication at: <https://www.researchgate.net/publication/289811185>

# On the Four-node Quadrilateral Element

Article · January 2011

DOI: 10.1007/978-3-642-17484-1\_6

---

CITATIONS

0

READS

2,711

2 authors, including:



Peter Wriggers

Leibniz Universität Hannover

933 PUBLICATIONS 18,190 CITATIONS

[SEE PROFILE](#)

Some of the authors of this publication are also working on these related projects:



ERC StG CA2PVM [View project](#)



Simulation and experimental testing of the collision behaviour of ships with double hulls filled with particles [View project](#)

# A FORMULATION FOR THE 4-NODE QUADRILATERAL ELEMENT

ULRICH HUECK AND PETER WRIGGERS

*Institut für Mechanik, Technische Hochschule Darmstadt, Hochschulstr. 1, 64289 Darmstadt, Germany*

‘Right things come in threes’

## SUMMARY

A formulation for the plane 4-node quadrilateral finite element is developed based on the principle of virtual displacements for a deformable body. Incompatible modes are added to the standard displacement field. Then expressions for gradient operators are obtained from an expansion of the basis functions into a second-order Taylor series in the physical co-ordinates. The internal degrees of freedom of the incompatible modes are eliminated on the element level. A modified change of variables is used to integrate the element matrices.

For a linear elastic material, the element stiffness matrix can be separated into two parts. These are equivalent to a stiffness matrix obtained from underintegration and a stabilization matrix.

The formulation includes the cases of plane stress and plane strain as well as the analysis of incompressible materials. Further, the approach is suitable for non-linear analysis. There, an application is given for the calculation of inelastic problems in physically non-linear elasticity.

The element is efficient to implement and it is frame invariant. Locking effects and zero-energy modes are avoided as well as singularities of the stiffness matrix due to geometric distortion. A high accuracy is obtained for numerical solutions in displacements and stresses.

**KEY WORDS:** quadrilateral; incompatible modes; underintegration; stabilization matrix

## 1. INTRODUCTION

Due to their simple geometry, 4-node quadrilateral elements are widely used for the finite element analysis of plane problems.

As is well known, for the quadrilateral, the standard isoparametric formulation as introduced by Taig<sup>1,2</sup> is not suitable for problems with coarse meshes or with meshes of high aspect ratios. For such application, the numerical accuracy of the element is low. As well, the standard element may not be used for the analysis of incompressible materials in plane strain. Furthermore, the standard element yields numerical singularities in the case of an extreme distortion of the element geometry.

Beside these disadvantages, the isoparametric formulation exhibits essential element properties: with a mesh refinement, the numerical solution converges to the exact solution. The element is rank sufficient and frame invariant. The formulation is based on a variational principle, the constitutive equation is incorporated in a rigorous fashion and an extension to non-linear applications can be made. Furthermore, the numerical effort to form the element stiffness matrix is comparably low.

Throughout the development of the finite element method, numerous efforts have been made to overcome the disadvantages of the isoparametric formulation without losing such essential element properties as described above.

Iron<sup>3</sup> indicates that a 1-point Gauss quadrature rule is sufficient to maintain convergence with mesh refinement for the quadrilateral. Based on some studies at the University of California, Berkeley,<sup>4</sup> Zienkiewicz *et al.*<sup>5</sup> and Pawsey and Clough<sup>6</sup> present approaches using reduced integration formulae for the evaluation of the element stiffness matrix. Immediate comments of Kavanagh and Key<sup>7</sup> indicate the necessity for a stabilization of the underintegrated quadrilateral. Then Kosloff and Frazier<sup>8</sup> propose a stabilization procedure in conjunction with the 1-point quadrature of the 4-node element. An explicit description for the element stabilization is developed by Flanagan and Belytschko,<sup>9,10</sup> referred to as the  $\gamma$ -stabilization of the quadrilateral. Later on several related stabilization procedures are proposed by Belytschko, Bachrach and Liu among others.<sup>11–24</sup> Here, Liu *et al.*<sup>14</sup> perform a Taylor series expansion in the natural co-ordinates of the bi-unit square for the element strain field, while Bachrach *et al.*<sup>19</sup> propose such expansion for the deviatoric part of the gradient operator. Further, an assumed stress field is utilized to construct a stabilization matrix.<sup>20</sup> The major advantage of stabilized elements may be observed in their robustness under extreme geometric distortion, making them more suitable for the analysis of problems involving large deformations. On the other hand, most of the stabilization procedures are not frame invariant, so that on the element level an additional transformation of co-ordinates is required.<sup>25,26</sup>

Wilson *et al.*<sup>27</sup> propose the use of additional incompatible basis functions. For a rectangular element geometry, significant improvements upon the standard isoparametric formulation are achieved. Fröier *et al.*<sup>28</sup> show that Wilson's formulation leads to an element equivalent to the one derived by Turner *et al.*,<sup>29</sup> which is probably the first quadrilateral presented in the literature.

But for a distorted geometry, the Wilson element turns out to violate the patch test for convergence. Taylor *et al.*<sup>30</sup> present a modified version of that element, leading to a high accuracy in the numerical solutions for displacement and stresses. At first glance, the two *ad hoc* modifications of the Wilson element are justified solely by the improvement of the element properties. Therefore, Strang and Fix<sup>31</sup> comment,

‘Two wrongs do make a right in California’.

Proposing a variationally consistent concept of assumed strains, Simo and Rifai<sup>32</sup> present a more rigorous derivation of the Taylor element. The reply to Strang and Fix is

‘Two rights make a right even in California’.

The formulation of Simo and Rifai includes the solution of problems involving inelastic materials. Then Simo and Armero<sup>33</sup> extend the assumed strain concept for the quadrilateral towards the analysis of geometrically non-linear problems.

Up to now, highest numerical accuracy is achieved with element formulations based on the classical assumed stress concept of Pian.<sup>34</sup> Here, the quadrilateral of Pian and Sumihara<sup>35</sup> is outstanding, on the one hand for its numerical accuracy, on the other hand for its efficiency when formulated in terms of a 1-point integration and a stabilization procedure.<sup>36,37</sup> While some later assumed stress approaches slightly improve upon the accuracy of that element,<sup>38–40</sup> its efficiency is not reached by these. As a major drawback, the assumed stress concept only allows for a complicated and cumbersome extension towards non-linear applications.<sup>32,36,41</sup>

Several other interesting approaches on the quadrilateral exist.<sup>42</sup> Some focus on the special treatment of the incompressible constraint,<sup>43–48</sup> others on the use of additional rotational degrees of freedom at the element nodes.<sup>49,50</sup>

In the present formulation, the incompatible modes introduced by Wilson *et al.*<sup>27</sup> are added to the standard element displacement field. Then the basis functions are expanded about the element centre into a second-order Taylor series<sup>51</sup> in the physical co-ordinates. The first-order terms of the Taylor series lead to a constant gradient operator, while the second-order terms are used to generate linear gradient operators. Through the evaluation of an equilibrium constraint, the internal degrees of freedom associated with the incompatible modes are eliminated on the element level. To provide for convergence with mesh refinement, a modified change of variables is used to integrate the element matrices. For a linear elastic material, the constant and the linear gradient operators are uncoupled. As a consequence, the element can be written in terms of a constant gradient matrix, usually obtained from 1-point integration, and a stabilization matrix.

The proposed quadrilateral overcomes the disadvantages of the Taig element, but keeps the essential properties of that standard formulation. Utilizing a 1-field variational principle, the approach unifies the concept of incompatible basis functions with the concept of underintegration and stabilization. For numerical solutions, the element achieves the accuracy of the established assumed stress elements. Further, the approach is suitable for non-linear analysis.

First, the element formulation is derived for the linear elastic case. A summary of the essential equations is given. Then, classical model problems are calculated. Results are compared with those obtained from existing formulations for the quadrilateral. Finally, an extension is made to incorporate the physically non-linear analysis of inelastic problems.

## 2. VARIATIONAL PRINCIPLE

The element formulation is based on the principle of virtual displacements for a deformable body:<sup>52</sup>

$$\delta W = \int \delta \boldsymbol{\epsilon}^T \boldsymbol{\sigma} dV - \delta W_{\text{ext}} = 0 \quad (2.1)$$

The integration is over the volume  $V$ ,  $\boldsymbol{\epsilon}$  is the strain field,  $\boldsymbol{\sigma}$  is the stress field and  $W_{\text{ext}}$  is the external virtual work of the specified surface tractions and of the body forces.

Additional displacement modes are added to the standard element displacement field. As a result, the element strain field is written as

$$\boldsymbol{\epsilon} = \mathbf{B}^T \mathbf{d} + \mathbf{G}^T \boldsymbol{\phi} \quad (2.2)$$

with the vector of nodal displacements,  $\mathbf{d}$ , the additional internal element degrees of freedom,  $\boldsymbol{\phi}$ , and the gradient operators  $\mathbf{B}$  and  $\mathbf{G}$ , being related to the standard shape functions and to the additional basis functions, respectively. The coefficients  $\boldsymbol{\phi}$  are assumed to contribute to the element strains but not to the external loads.<sup>30,32</sup> With  $\mathbf{d}$  and  $\boldsymbol{\phi}$  independent, equation (2.1) yields a relation  $\boldsymbol{\phi} = \boldsymbol{\phi}(\mathbf{d})$  so that the internal coefficients  $\boldsymbol{\phi}$  can be eliminated on the element level.

The variation in the strain field

$$\delta \boldsymbol{\epsilon} = \mathbf{B}^T \delta \mathbf{d} + \mathbf{G}^T \delta \boldsymbol{\phi} \quad (2.3)$$

is introduced into (2.1) and leads to

$$\delta \mathbf{d}^T \int \mathbf{B} \boldsymbol{\sigma} dV + \delta \boldsymbol{\phi}^T \int \mathbf{G} \boldsymbol{\sigma} dV - \delta W_{\text{ext}} = 0 \quad (2.4)$$

which must hold for all variations in  $\delta \mathbf{d}$  and  $\delta \boldsymbol{\phi}$ . The virtual work of the external loading

$$\delta W_{\text{ext}} = \delta \mathbf{d}^T \mathbf{f} \quad (2.5)$$

is independent of a variation in  $\delta\phi$ , since the load vector  $\mathbf{f}$  is only related to the nodes of the element. Therefore, the resulting equations for the finite element approximation are

$$\int \mathbf{B} \sigma dV - \mathbf{f} = \mathbf{0} \quad (2.6)$$

$$\int \mathbf{G} \sigma dV = \mathbf{0} \quad (2.7)$$

### 3. LINEAR ELASTIC MATERIAL

For a linear elastic material the constitutive equation is

$$\sigma = \mathbf{E} \varepsilon \quad (3.1)$$

where  $\mathbf{E}$  denotes the matrix of material stiffnesses. In the case of an isotropic, plane, 2-dimensional problem

$$\sigma = \begin{pmatrix} \sigma_x \\ \sigma_y \\ \tau_{xy} \end{pmatrix} \quad \mathbf{E} = \begin{pmatrix} E_1 & E_2 & 0 \\ E_2 & E_1 & 0 \\ 0 & 0 & G \end{pmatrix} \quad \varepsilon = \begin{pmatrix} \varepsilon_x \\ \varepsilon_y \\ \gamma_{xy} \end{pmatrix} \quad (3.2)$$

For plane stress,

$$E_1 = \frac{E}{1 - \nu^2} \quad E_2 = \nu E_1 \quad (3.3)$$

while for plane strain,

$$E_1 = \frac{E(1 - \nu)}{(1 + \nu)(1 - 2\nu)} \quad E_2 = \frac{\nu E_1}{1 - \nu} \quad (3.4)$$

with Young's modulus  $E$ , Poisson's ratio  $\nu$  and the shear modulus  $G = E/(2 + 2\nu)$ .

Introducing (3.1) and (3.2) into (2.6) and (2.7) leads to the two equations

$$\left( \int \mathbf{B} \mathbf{E} \mathbf{B}^T dV \right) \mathbf{d} + \left( \int \mathbf{B} \mathbf{E} \mathbf{G}^T dV \right) \phi = \mathbf{f} \quad (3.5)$$

$$\left( \int \mathbf{G} \mathbf{E} \mathbf{B}^T dV \right) \mathbf{d} + \left( \int \mathbf{G} \mathbf{E} \mathbf{G}^T dV \right) \phi = \mathbf{0} \quad (3.6)$$

On the element level, the evaluation of (3.6) yields the relation

$$\phi = \phi(\mathbf{d}) \quad (3.7)$$

In the classical approach, the element stiffness matrix is obtained from (3.5) and (3.6) where the coefficients  $\phi$  are condensed out on the element level.<sup>27,30</sup> The resulting system of equations is

$$\mathbf{K} \mathbf{d} = \mathbf{f} \quad (3.8)$$

with the modified element stiffness matrix

$$\mathbf{K} = \left( \int \mathbf{B} \mathbf{E} \mathbf{B}^T dV \right) - \left( \int \mathbf{B} \mathbf{E} \mathbf{G}^T dV \right) \left( \int \mathbf{G} \mathbf{E} \mathbf{G}^T dV \right)^{-1} \left( \int \mathbf{G} \mathbf{E} \mathbf{B}^T dV \right) \quad (3.9)$$

As an alternative, (3.7) can be used to form a complete gradient operator  $\bar{\mathbf{B}}$ :<sup>46,47</sup>

$$\boldsymbol{\varepsilon} = \mathbf{B}^T \mathbf{d} + \mathbf{G}^T \boldsymbol{\varphi}(\mathbf{d}) = \bar{\mathbf{B}}^T \mathbf{d} \quad (3.10)$$

Then from (2.1), (3.1) and (3.10), the element stiffness matrix is obtained as

$$\mathbf{K} = \int \bar{\mathbf{B}} \mathbf{E} \bar{\mathbf{B}}^T dV \quad (3.11)$$

#### 4. KINEMATICS

The vector of nodal displacements,  $\mathbf{d}$ , is written in terms of its components  $\mathbf{u}$  and  $\mathbf{v}$  in the  $x$ - and in the  $y$ -direction, respectively:

$$\mathbf{d} = \begin{pmatrix} \mathbf{u} \\ \mathbf{v} \end{pmatrix} \quad \mathbf{u}^T = (u_1 \ u_2 \ u_3 \ u_4) \quad \mathbf{v}^T = (v_1 \ v_2 \ v_3 \ v_4) \quad (4.1)$$

Then the element displacement field is described by means of the standard bilinear shape function  $\mathbf{n}$ :

$$u = \mathbf{n}^T \mathbf{u} + \mathbf{w}^T \begin{pmatrix} \varphi_1 \\ \varphi_2 \end{pmatrix} \quad v = \mathbf{n}^T \mathbf{v} + \mathbf{w}^T \begin{pmatrix} \varphi_3 \\ \varphi_4 \end{pmatrix} \quad (4.2)$$

Here, the incompatible modes<sup>27</sup>

$$\mathbf{w} = \begin{pmatrix} 1 - \xi^2 \\ 1 - \eta^2 \end{pmatrix} \quad (4.3)$$

are added in conjunction with the internal element degrees of freedom

$$\boldsymbol{\varphi}^T = (\varphi_1 \ \varphi_2 \ \varphi_3 \ \varphi_4) \quad (4.4)$$

Then the element strain field may be expressed through

$$\boldsymbol{\varepsilon} = \begin{pmatrix} \varepsilon_x \\ \varepsilon_y \\ \gamma_{xy} \end{pmatrix} = \begin{pmatrix} \frac{\partial \mathbf{n}^T}{\partial x} & \mathbf{0} \\ \mathbf{0} & \frac{\partial \mathbf{n}^T}{\partial y} \\ \frac{\partial \mathbf{n}^T}{\partial y} & \frac{\partial \mathbf{n}^T}{\partial x} \end{pmatrix} \begin{pmatrix} \mathbf{u} \\ \mathbf{v} \end{pmatrix} + \begin{pmatrix} \frac{\partial \mathbf{w}^T}{\partial x} & \mathbf{0} \\ \mathbf{0} & \frac{\partial \mathbf{w}^T}{\partial y} \\ \frac{\partial \mathbf{w}^T}{\partial y} & \frac{\partial \mathbf{w}^T}{\partial x} \end{pmatrix} \begin{pmatrix} \varphi_1 \\ \varphi_2 \\ \varphi_3 \\ \varphi_4 \end{pmatrix} \quad (4.5)$$

In the present formulation, the derivatives of the basis functions  $\mathbf{n}$  and  $\mathbf{w}$  in (4.5) will be approximated through a Taylor series expansion about the element centre.

The standard bilinear element shape functions are separated into constant, linear and bilinear parts by setting

$$\mathbf{n} = \frac{1}{4} \begin{pmatrix} (1 - \xi)(1 - \eta) \\ (1 + \xi)(1 - \eta) \\ (1 + \xi)(1 + \eta) \\ (1 - \xi)(1 + \eta) \end{pmatrix} = \frac{1}{2} (\mathbf{r} + \mathbf{g}_\xi \xi + \mathbf{g}_\eta \eta + \mathbf{h} \xi \eta) \quad (4.6)$$

with

$$\mathbf{r} = \frac{1}{2} \begin{pmatrix} 1 \\ 1 \\ 1 \\ 1 \end{pmatrix} \quad \mathbf{g}_\xi = \frac{1}{2} \begin{pmatrix} -1 \\ 1 \\ 1 \\ -1 \end{pmatrix} \quad \mathbf{g}_\eta = \frac{1}{2} \begin{pmatrix} -1 \\ -1 \\ 1 \\ 1 \end{pmatrix} \quad \mathbf{h} = \frac{1}{2} \begin{pmatrix} 1 \\ -1 \\ 1 \\ -1 \end{pmatrix} \quad (4.7)$$

where  $\mathbf{r}$ ,  $\mathbf{g}$  and  $\mathbf{h}$  stand for ‘rigid body’, ‘constant gradient’, and ‘hourglass’, respectively.<sup>53</sup> The co-ordinates of the element nodes are

$$\mathbf{x}^T = (x_1 \ x_2 \ x_3 \ x_4) \quad \mathbf{y}^T = (y_1 \ y_2 \ y_3 \ y_4) \quad (4.8)$$

From these, constant element coefficients are defined<sup>35</sup> by using the vectors of the element shape functions in (4.7):

$$\begin{pmatrix} a_0 & b_0 \\ a_1 & b_1 \\ a_2 & b_2 \\ a_3 & b_3 \end{pmatrix} = \frac{1}{2} \begin{pmatrix} \mathbf{r}^T \\ \mathbf{g}_\xi^T \\ \mathbf{h}^T \\ \mathbf{g}_\eta^T \end{pmatrix} (\mathbf{x} \ \mathbf{y}) = \frac{1}{4} \begin{pmatrix} 1 & 1 & 1 & 1 \\ -1 & 1 & 1 & -1 \\ 1 & -1 & 1 & -1 \\ -1 & -1 & 1 & 1 \end{pmatrix} \begin{pmatrix} x_1 & y_1 \\ x_2 & y_2 \\ x_3 & y_3 \\ x_4 & y_4 \end{pmatrix} \quad (4.9)$$

Then the transformation of the element co-ordinates is

$$\begin{aligned} x &= \mathbf{x}^T \mathbf{n} = a_0 + a_1 \xi + a_2 \xi \eta + a_3 \eta \\ y &= \mathbf{y}^T \mathbf{n} = b_0 + b_1 \xi + b_2 \xi \eta + b_3 \eta \end{aligned} \quad (4.10)$$

A geometric interpretation of the coefficients  $a_0 \dots b_3$  is given by Robinson.<sup>54</sup> The mapping of the 4-node quadrilateral element from the physical space into the master element space is shown in Figure 1.

The relation between the derivatives of the element shape functions with respect to the co-ordinates of the mapping,  $\xi$  and  $\eta$ , and with respect to the physical co-ordinates,  $x$  and  $y$ , is given by the chain rule

$$\begin{pmatrix} \frac{\partial \mathbf{n}^T}{\partial \xi} \\ \frac{\partial \mathbf{n}^T}{\partial \eta} \end{pmatrix} = \begin{pmatrix} \frac{\partial x}{\partial \xi} & \frac{\partial y}{\partial \xi} \\ \frac{\partial x}{\partial \eta} & \frac{\partial y}{\partial \eta} \end{pmatrix} \begin{pmatrix} \frac{\partial \mathbf{n}^T}{\partial x} \\ \frac{\partial \mathbf{n}^T}{\partial y} \end{pmatrix} \quad (4.11)$$

The derivatives

$$\frac{\partial \mathbf{n}}{\partial \xi} = \frac{1}{2}(\mathbf{g}_\xi + \mathbf{h} \eta) \quad \frac{\partial \mathbf{n}}{\partial \eta} = \frac{1}{2}(\mathbf{g}_\eta + \mathbf{h} \xi) \quad (4.12)$$

are obtained directly from (4.6). Equation (4.11) contains the Jacobian of the mapping

$$\mathbf{J} = \begin{pmatrix} \frac{\partial x}{\partial \xi} & \frac{\partial y}{\partial \xi} \\ \frac{\partial x}{\partial \eta} & \frac{\partial y}{\partial \eta} \end{pmatrix} = \begin{pmatrix} a_1 + a_2 \eta & b_1 + b_2 \eta \\ a_3 + a_2 \xi & b_3 + b_2 \xi \end{pmatrix} \quad (4.13)$$

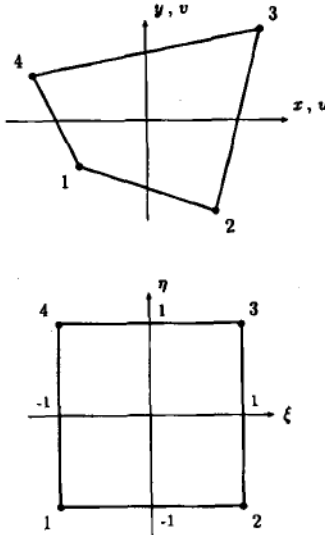


Figure 1. Mapping of 4-node quadrilateral element

Its determinant is

$$J = \det \mathbf{J} = J_0 + J_1 \xi + J_2 \eta \quad (4.14)$$

with the constant coefficients

$$\begin{aligned} J_0 &= a_1 b_3 - a_3 b_1 \\ J_1 &= a_1 b_2 - a_2 b_1 \\ J_2 &= a_2 b_3 - a_3 b_2 \end{aligned} \quad (4.15)$$

The inverse relationship for the derivatives of the element shape functions is

$$\begin{pmatrix} \frac{\partial \mathbf{n}^T}{\partial x} \\ \frac{\partial \mathbf{n}^T}{\partial y} \end{pmatrix} = \begin{pmatrix} \frac{\partial \xi}{\partial x} & \frac{\partial \eta}{\partial x} \\ \frac{\partial \xi}{\partial y} & \frac{\partial \eta}{\partial y} \end{pmatrix} \begin{pmatrix} \frac{\partial \mathbf{n}^T}{\partial \xi} \\ \frac{\partial \mathbf{n}^T}{\partial \eta} \end{pmatrix} \quad (4.16)$$

Equation (4.16) contains the inverse of the Jacobian:

$$\mathbf{J}^{-1} = \frac{1}{J} \begin{pmatrix} \frac{\partial y}{\partial \eta} & -\frac{\partial y}{\partial \xi} \\ -\frac{\partial x}{\partial \eta} & \frac{\partial x}{\partial \xi} \end{pmatrix} = \frac{1}{J} \begin{pmatrix} (b_3 + b_2 \xi) & -(b_1 + b_2 \eta) \\ -(a_3 + a_2 \xi) & (a_1 + a_2 \eta) \end{pmatrix} \quad (4.17)$$

Then the derivatives of the co-ordinates of the mapping with respect to  $x$  and  $y$  are obtained from (4.16) and (4.17) as

$$\frac{\partial \xi}{\partial x} = -\frac{1}{J}(b_3 + b_2 \xi) \quad \frac{\partial \xi}{\partial y} = -\frac{1}{J}(a_3 + a_2 \xi) \quad (4.18)$$

$$\frac{\partial \eta}{\partial x} = -\frac{1}{J}(b_1 + b_2 \eta) \quad \frac{\partial \eta}{\partial y} = \frac{1}{J}(a_1 + a_2 \eta)$$

Finally, application of the product rule and the chain rule leads to

$$\begin{aligned}\frac{\partial \xi \eta}{\partial x} &= \frac{1}{J} (b_3 \eta - b_1 \xi) & \frac{\partial \xi \eta}{\partial y} &= \frac{1}{J} (a_1 \xi - a_3 \eta) \\ \frac{\partial \xi^2}{\partial x} &= \frac{2\xi}{J} (b_3 + b_2 \xi) & \frac{\partial \xi^2}{\partial y} &= -\frac{2\xi}{J} (a_3 + a_2 \xi) \\ \frac{\partial \eta^2}{\partial x} &= -\frac{2\eta}{J} (b_1 + b_2 \eta) & \frac{\partial \eta^2}{\partial y} &= \frac{2\eta}{J} (a_1 + a_2 \eta)\end{aligned}\quad (4.19)$$

## 5. TAYLOR SERIES

The standard isoparametric shape functions may be expanded about the element centre into a complete first-order Taylor series in the physical co-ordinates,  $x$  and  $y$ . Then the remaining higher-order term is of the type  $\xi\eta$ . The first-order terms lead to a constant gradient operator. This operator is also involved when using a 1-point quadrature rule for the evaluation of the standard element stiffness matrix. A stabilization matrix is related to the remaining higher-order term.

For an underintegrated and stabilized element, the convergence with mesh refinement is almost independent of the parameters used for the stabilization over a wide range of values.<sup>12</sup> Therefore, the convergence property of the quadrilateral is traced back to the first-order terms of a Taylor series of the shape functions. Consequently, additional quadratic modes are added to the remaining bilinear term of higher order, all of these being expanded into a second-order Taylor series. Remaining terms of third order are neglected. Figure 2 illustrates the situation for the standard element, called Q4, and for the approach proposed here.

With the second-order terms being uncoupled from the first-order terms, the resulting element stiffness matrix can be written as an underintegrated matrix and a stabilization matrix.

The procedure outlined unifies the concept of incompatible modes, where six basis functions are used, with the concept of stabilization. Therefore, the new element is called QS6.

$$\begin{array}{ccc} & & 1 \\ & & \\ \xi & \eta & = \\ 0 & \xi\eta & 0 & 0 & \xi\eta & 0 \\ & & & & & \\ & & 1 & & 1 \\ & & & \Rightarrow & & \\ & & \xi & \eta & & x & y \\ & & \xi^2 & \xi\eta & \eta^2 & x^2 & xy & y^2 \end{array}$$

Figure 2. Pascal's triangles for the Q4 element and for the QS6 element

### 5.1. First-order terms

**5.1.1. Shape functions.** In the physical co-ordinates, the element shape functions are expanded into a first-order Taylor series. The expansion point is the element centre with the co-ordinates

$$x_0 = x(\xi = 0, \eta = 0) \quad y_0 = y(\xi = 0, \eta = 0) \quad (5.1)$$

Then the Taylor series is

$$\mathbf{n} = \mathbf{n}|_0 + \left. \frac{\partial \mathbf{n}}{\partial x} \right|_0 (x - x_0) + \left. \frac{\partial \mathbf{n}}{\partial y} \right|_0 (y - y_0) + \mathbf{n}_\gamma \quad (5.2)$$

with the remaining higher-order terms  $\mathbf{n}_\gamma$ . The constant term in (5.2) is obtained from (4.6):

$$\mathbf{n}|_0 = \frac{1}{2} \mathbf{r} \quad (5.3)$$

To calculate the first-order derivatives of the shape functions with respect to the physical co-ordinates, equation (4.16) is evaluated at  $\xi = 0, \eta = 0$ :

$$\begin{pmatrix} \left. \frac{\partial \mathbf{n}}{\partial x} \right|_0^T \\ \left. \frac{\partial \mathbf{n}}{\partial y} \right|_0^T \end{pmatrix} = \mathbf{J}|_0^{-1} \begin{pmatrix} \left. \frac{\partial \mathbf{n}}{\partial \xi} \right|_0^T \\ \left. \frac{\partial \mathbf{n}}{\partial \eta} \right|_0^T \end{pmatrix} \quad (5.4)$$

where the inverse of the Jacobian at the element centre is obtained from (4.17) as

$$\mathbf{J}_0^{-1} = \mathbf{J}|_0^{-1} = \frac{1}{J_0} \begin{pmatrix} b_3 & -b_1 \\ -a_3 & a_1 \end{pmatrix} \quad (5.5)$$

The evaluation of (4.12) at the element centre yields the derivatives of the shape functions with respect to  $\xi$  and  $\eta$ :

$$\left. \frac{\partial \mathbf{n}}{\partial \xi} \right|_0 = \frac{1}{2} \mathbf{g}_\xi \quad \left. \frac{\partial \mathbf{n}}{\partial \eta} \right|_0 = \frac{1}{2} \mathbf{g}_\eta \quad (5.6)$$

Introducing (5.6) and (5.5) into (5.4) leads to expressions for the derivatives of the shape functions with respect to the physical co-ordinates at the element centre:

$$\left. \frac{\partial \mathbf{n}}{\partial x} \right|_0 = \frac{1}{2J_0} (b_3 \mathbf{g}_\xi - b_1 \mathbf{g}_\eta) \quad (5.7)$$

$$\left. \frac{\partial \mathbf{n}}{\partial y} \right|_0 = \frac{1}{2J_0} (a_1 \mathbf{g}_\eta - a_3 \mathbf{g}_\xi)$$

The term  $\mathbf{n}_\gamma$  in (5.2) will now be obtained by subtracting from the shape functions themselves the constant term and the first-order terms of the Taylor series:

$$\mathbf{n}_\gamma = \mathbf{n} - \mathbf{n}|_0 - \left( \left. \frac{\partial \mathbf{n}}{\partial x} \right|_0 \quad \left. \frac{\partial \mathbf{n}}{\partial y} \right|_0 \right) \begin{pmatrix} x - x_0 \\ y - y_0 \end{pmatrix} \quad (5.8)$$

Equations (4.10) and (5.1) yield

$$\begin{pmatrix} x - x_0 \\ y - y_0 \end{pmatrix} = \begin{pmatrix} \Delta x \\ \Delta y \end{pmatrix} = \begin{pmatrix} a_1 & a_2 & a_3 \\ b_1 & b_2 & b_3 \end{pmatrix} \begin{pmatrix} \xi \\ \eta \\ \eta \end{pmatrix} \quad (5.9)$$

As an alternative, (4.10) leads to

$$\begin{pmatrix} x - x_0 \\ y - y_0 \end{pmatrix} = \begin{pmatrix} \mathbf{x}^T \\ \mathbf{y}^T \end{pmatrix} (\mathbf{n} - \mathbf{n}|_0) \quad (5.10)$$

Using (5.6), the derivatives in (5.8) may be expressed through the transposed form of (5.4):

$$\left( \frac{\partial \mathbf{n}}{\partial x} \Big|_0 \quad \frac{\partial \mathbf{n}}{\partial y} \Big|_0 \right) = \left( \frac{\partial \mathbf{n}}{\partial \xi} \Big|_0 \quad \frac{\partial \mathbf{n}}{\partial \eta} \Big|_0 \right) \mathbf{J}_0^{-T} = \frac{1}{2} (\mathbf{g}_\xi \quad \mathbf{g}_\eta) \mathbf{J}_0^{-T} \quad (5.11)$$

Introducing (5.10) and (5.11) into (5.8) yields

$$\mathbf{n}_\gamma = (\mathbf{n} - \mathbf{n}|_0) - \frac{1}{2} (\mathbf{g}_\xi \quad \mathbf{g}_\eta) \mathbf{J}_0^{-T} \begin{pmatrix} \mathbf{x}^T \\ \mathbf{y}^T \end{pmatrix} (\mathbf{n} - \mathbf{n}|_0) \quad (5.12)$$

With (4.6) and (5.3) one may write

$$\mathbf{n} - \mathbf{n}|_0 = \frac{1}{2} \left[ (\mathbf{g}_\xi \quad \mathbf{g}_\eta) \begin{pmatrix} \xi \\ \eta \end{pmatrix} + \mathbf{h} \xi \eta \right] \quad (5.13)$$

Then (5.13) is introduced into (5.12) to obtain

$$\mathbf{n}_\gamma = \frac{1}{2} \left[ (\mathbf{g}_\xi \quad \mathbf{g}_\eta) \begin{pmatrix} \xi \\ \eta \end{pmatrix} + \mathbf{h} \xi \eta \right] - \frac{1}{2} \left[ (\mathbf{g}_\xi \quad \mathbf{g}_\eta) \mathbf{J}_0^{-T} \begin{pmatrix} \mathbf{x}^T \\ \mathbf{y}^T \end{pmatrix} \right] \frac{1}{2} \left[ (\mathbf{g}_\xi \quad \mathbf{g}_\eta) \begin{pmatrix} \xi \\ \eta \end{pmatrix} + \mathbf{h} \xi \eta \right] \quad (5.14)$$

From (4.13) and (4.9) one finds

$$\mathbf{J}_0^T = \begin{pmatrix} a_1 & a_3 \\ b_1 & b_3 \end{pmatrix} = \frac{1}{2} \begin{pmatrix} \mathbf{x}^T \\ \mathbf{y}^T \end{pmatrix} (\mathbf{g}_\xi \quad \mathbf{g}_\eta) \quad (5.15)$$

Therefore, in (5.14) one expression is simplified to

$$\mathbf{J}_0^{-T} \begin{pmatrix} \mathbf{x}^T \\ \mathbf{y}^T \end{pmatrix} \frac{1}{2} (\mathbf{g}_\xi \quad \mathbf{g}_\eta) \begin{pmatrix} \xi \\ \eta \end{pmatrix} = \mathbf{J}_0^{-T} \mathbf{J}_0^T \begin{pmatrix} \xi \\ \eta \end{pmatrix} = \begin{pmatrix} \xi \\ \eta \end{pmatrix}$$

Furthermore, the use of (5.5), (4.9) and (4.15) leads to

$$\mathbf{J}_0^{-T} \begin{pmatrix} \mathbf{x}^T \\ \mathbf{y}^T \end{pmatrix} \frac{1}{2} \mathbf{h} \xi \eta = \frac{1}{J_0} \begin{pmatrix} b_3 & -a_3 \\ -b_1 & a_1 \end{pmatrix} \begin{pmatrix} a_2 \\ b_2 \end{pmatrix} \xi \eta = \frac{1}{J_0} \begin{pmatrix} J_2 \\ J_1 \end{pmatrix} \xi \eta$$

As a consequence, equation (5.14) can be rewritten as

$$\begin{aligned} \mathbf{n}_\gamma = & \frac{1}{2} (\mathbf{g}_\xi \quad \mathbf{g}_\eta) \begin{pmatrix} \xi \\ \eta \end{pmatrix} + \frac{1}{2} \mathbf{h} \xi \eta \\ & - \frac{1}{2} (\mathbf{g}_\xi \quad \mathbf{g}_\eta) \left[ \begin{pmatrix} \xi \\ \eta \end{pmatrix} + \frac{1}{J_0} \begin{pmatrix} J_2 \\ J_1 \end{pmatrix} \xi \eta \right] \end{aligned} \quad (5.16)$$

Then the higher-order term takes the simple form

$$\mathbf{n}_\gamma = \boldsymbol{\gamma} \xi \eta \quad (5.17)$$

with the  $\boldsymbol{\gamma}$ -vector<sup>9,55</sup>

$$\boldsymbol{\gamma} = \frac{1}{2} \left( \mathbf{h} - \frac{J_2}{J_0} \mathbf{g}_\xi - \frac{J_1}{J_0} \mathbf{g}_\eta \right) \quad (5.18)$$

**5.1.2. Incompatible modes.** The first-order Taylor series expansion of the incompatible basis functions

$$\mathbf{w} = \begin{pmatrix} 1 - \xi^2 \\ 1 - \eta^2 \end{pmatrix} \quad (4.3)$$

is

$$\mathbf{w} = \mathbf{w}|_0 + \frac{\partial \mathbf{w}}{\partial x} \Big|_0 (x - x_0) + \frac{\partial \mathbf{w}}{\partial y} \Big|_0 (y - y_0) + \mathbf{w}_\gamma \quad (5.19)$$

with the higher-order term  $\mathbf{w}_\gamma$ . The constant part of this Taylor series is

$$\mathbf{w}|_0^T = (1 \quad 1) \quad (5.20)$$

According to (4.19), the first-order terms are zero:

$$\left( \frac{\partial \mathbf{w}}{\partial x} \Big|_0 \quad \frac{\partial \mathbf{w}}{\partial y} \Big|_0 \right) = - \left( \begin{matrix} \frac{\partial \xi^2}{\partial x} \Big|_0 & \frac{\partial \xi^2}{\partial y} \Big|_0 \\ \frac{\partial \eta^2}{\partial x} \Big|_0 & \frac{\partial \eta^2}{\partial y} \Big|_0 \end{matrix} \right) = \mathbf{0} \quad (5.21)$$

Therefore, the higher-order term is

$$\mathbf{w}_\gamma^T = -(\xi^2 \quad \eta^2) \quad (5.22)$$

## 5.2. Second-order terms

The higher-order terms as obtained in (5.17) and (5.22)

$$\mathbf{n}_\gamma = \boldsymbol{\gamma} \xi \eta \quad \mathbf{w}_\gamma^T = -(\xi^2 \quad \eta^2) \quad (5.23)$$

are expanded into a second-order Taylor series. Therefore, the vector

$$\mathbf{p}^T = (p_1 \ p_2 \ p_3) = (\xi^2 \ \xi \eta \ \eta^2) \quad (5.24)$$

is introduced, containing the corresponding functions in (5.23). Its Taylor series expansion is

$$\mathbf{p} = \frac{1}{2} \left( \frac{\partial^2 \mathbf{p}}{\partial x^2} \Big|_0 \Delta x^2 + 2 \frac{\partial^2 \mathbf{p}}{\partial x \partial y} \Big|_0 \Delta x \Delta y + \frac{\partial^2 \mathbf{p}}{\partial y^2} \Big|_0 \Delta y^2 \right) + \mathbf{r}_3 \quad (5.25)$$

because the elements of  $\mathbf{p}$  already describe higher-order terms in the Taylor series expansions. The remaining term of third order is labeled  $\mathbf{r}_3$ . For the following derivation, indicial notation and the summation convention are used. The second-order derivatives of  $p_m$  with respect to  $x_i$ , with

$x_1 = x$  and  $x_2 = y$ , are obtained from the second-order derivatives of  $p_m$  with respect to  $\xi_j$ , with  $\xi_1 = \xi$  and  $\xi_2 = \eta$ . Using the chain rule, the first derivatives with respect to  $\xi_j$  are

$$\frac{\partial p_m}{\partial \xi_j} = \frac{\partial p_m}{\partial x_i} \frac{\partial x_i}{\partial \xi_j} \quad (5.26)$$

Further differentiation with respect to  $\xi_k$  leads to

$$\frac{\partial^2 p_m}{\partial \xi_k \partial \xi_j} = \frac{\partial^2 p_m}{\partial x_i \partial x_i} \frac{\partial x_i}{\partial \xi_k} \frac{\partial x_i}{\partial \xi_j} + \frac{\partial p_m}{\partial x_i} \frac{\partial^2 x_i}{\partial \xi_k \partial \xi_j} \quad (5.27)$$

According to (4.19), at the element centre the first derivatives of  $p_m$  with respect to  $x_i$  are zero

$$\left. \frac{\partial p_m}{\partial x_i} \right|_0 = 0 \quad (5.28)$$

Then in matrix form the remaining terms at the element centre are

$$\begin{pmatrix} \frac{\partial^2 \mathbf{p}^T}{\partial \xi^2} \\ \frac{\partial^2 \mathbf{p}^T}{\partial \xi \partial \eta} \\ \frac{\partial^2 \mathbf{p}^T}{\partial \eta^2} \end{pmatrix}_0 = \begin{pmatrix} \left( \frac{\partial x}{\partial \xi} \right)^2 & 2 \left( \frac{\partial x}{\partial \xi} \frac{\partial y}{\partial \xi} \right) & \left( \frac{\partial y}{\partial \xi} \right)^2 \\ \left( \frac{\partial x}{\partial \xi} \frac{\partial x}{\partial \eta} \right) & \left( \frac{\partial x}{\partial \xi} \frac{\partial y}{\partial \eta} + \frac{\partial y}{\partial \xi} \frac{\partial x}{\partial \eta} \right) & \left( \frac{\partial y}{\partial \xi} \frac{\partial y}{\partial \eta} \right) \\ \left( \frac{\partial x}{\partial \eta} \right)^2 & 2 \left( \frac{\partial x}{\partial \eta} \frac{\partial y}{\partial \eta} \right) & \left( \frac{\partial y}{\partial \eta} \right)^2 \end{pmatrix}_0 \begin{pmatrix} \frac{\partial^2 \mathbf{p}^T}{\partial x^2} \\ \frac{\partial^2 \mathbf{p}^T}{\partial x \partial y} \\ \frac{\partial^2 \mathbf{p}^T}{\partial y^2} \end{pmatrix}_0 \quad (5.29)$$

With (4.13), the transformation matrix in (5.29) is obtained as

$$\mathbf{P}_0 = \begin{pmatrix} a_1^2 & 2a_1 b_1 & b_1^2 \\ a_1 a_3 & a_1 b_3 + a_3 b_1 & b_1 b_3 \\ a_3^2 & 2a_3 b_3 & b_3^2 \end{pmatrix} \quad (5.30)$$

Using (4.15), its determinant is

$$\det \mathbf{P}_0 = J_0^3 \quad (5.31)$$

and its inverse is

$$\mathbf{P}_0^{-1} = \frac{1}{J_0^2} \begin{pmatrix} b_3^2 & -2b_1 b_3 & b_1^2 \\ -a_3 b_3 & a_1 b_3 + a_3 b_1 & -a_1 b_1 \\ a_3^2 & -2a_1 a_3 & a_1^2 \end{pmatrix} \quad (5.32)$$

On the other hand, differentiating (5.24) twice with respect to  $\xi$  and  $\eta$  yields

$$\begin{pmatrix} \frac{\partial^2 \mathbf{p}}{\partial \xi^2} & \frac{\partial^2 \mathbf{p}}{\partial \xi \partial \eta} & \frac{\partial^2 \mathbf{p}}{\partial \eta^2} \end{pmatrix}_0 = \begin{pmatrix} 2 & 0 & 0 \\ 0 & 1 & 0 \\ 0 & 0 & 2 \end{pmatrix} \quad (5.33)$$

Equation (5.29) is solved by introduction of (5.33) and by multiplication with  $\mathbf{P}_0^{-1}$ . Then at the element centre the second derivatives of the functions  $\xi^2$ ,  $\xi\eta$  and  $\eta^2$  with respect to  $x$  and  $y$  are

$$\begin{pmatrix} \frac{\partial^2 \xi^2}{\partial x^2} \Big|_0 & \frac{\partial^2 \xi\eta}{\partial x^2} \Big|_0 & \frac{\partial^2 \eta^2}{\partial x^2} \Big|_0 \\ \frac{\partial^2 \xi^2}{\partial x \partial y} \Big|_0 & \frac{\partial^2 \xi\eta}{\partial x \partial y} \Big|_0 & \frac{\partial^2 \eta^2}{\partial x \partial y} \Big|_0 \\ \frac{\partial^2 \xi^2}{\partial y^2} \Big|_0 & \frac{\partial^2 \xi\eta}{\partial y^2} \Big|_0 & \frac{\partial^2 \eta^2}{\partial y^2} \Big|_0 \end{pmatrix} = \frac{1}{J_0^2} \begin{pmatrix} 2b_3^2 & -2b_1b_3 & 2b_1^2 \\ -2a_3b_3 & a_1b_3 + a_3b_1 & -2a_1b_1 \\ 2a_3^2 & -2a_1a_3 & 2a_1^2 \end{pmatrix} \quad (5.34)$$

According to (5.25), noting the signs in (5.23) and using (5.34), the formulae for the higher-order terms  $\mathbf{n}_\gamma$  and  $\mathbf{w}_\gamma$  are finally obtained as

$$\mathbf{n}_\gamma = -\frac{1}{J_0^2} (b_1b_3\Delta x^2 - (a_1b_3 + a_3b_1)\Delta x\Delta y + a_1a_3\Delta y^2)\boldsymbol{\gamma} + \mathbf{r}_3 \quad (5.35)$$

$$\mathbf{w}_\gamma = -\frac{1}{J_0^2} \begin{pmatrix} b_3^2\Delta x^2 - 2a_3b_3\Delta x\Delta y + a_3^2\Delta y^2 \\ b_1^2\Delta x^2 - 2a_1b_1\Delta x\Delta y + a_1^2\Delta y^2 \end{pmatrix} + \mathbf{r}_3 \quad (5.36)$$

Subsequently, the terms of third order,  $\mathbf{r}_3$ , will be neglected.

## 6. GRADIENT OPERATORS

As described in (4.5), the gradient operators  $\mathbf{B}$  and  $\mathbf{G}$  from (2.2) contain the derivatives of the element basis functions. These will be approximated by the Taylor series expansion.

Differentiation of (5.2) with respect to  $x$  and  $y$  yields

$$\begin{aligned} \begin{pmatrix} \frac{\partial \mathbf{n}}{\partial x} \\ \frac{\partial \mathbf{n}}{\partial y} \end{pmatrix} &= \begin{pmatrix} \frac{\partial \mathbf{n}}{\partial x} \Big|_0 \\ \frac{\partial \mathbf{n}}{\partial y} \Big|_0 \end{pmatrix} + \begin{pmatrix} \frac{\partial \mathbf{n}_\gamma^T}{\partial x} \\ \frac{\partial \mathbf{n}_\gamma^T}{\partial y} \end{pmatrix} \\ &= \frac{1}{2J_0} \begin{pmatrix} b_3 & -b_1 \\ -a_3 & a_1 \end{pmatrix} \begin{pmatrix} \mathbf{g}_\xi^T \\ \mathbf{g}_\eta^T \end{pmatrix} + \begin{pmatrix} \frac{\partial \mathbf{n}_\gamma^T}{\partial x} \\ \frac{\partial \mathbf{n}_\gamma^T}{\partial y} \end{pmatrix} \end{aligned} \quad (6.1)$$

where (5.7) is used. Further, differentiating (5.35) leads to

$$\begin{pmatrix} \frac{\partial \mathbf{n}_\gamma^T}{\partial x} \\ \frac{\partial \mathbf{n}_\gamma^T}{\partial y} \end{pmatrix} = \frac{1}{J_0^2} \begin{pmatrix} -2b_1b_3 & (a_1b_3 + a_3b_1) \\ (a_1b_3 + a_3b_1) & -2a_1a_3 \end{pmatrix} \begin{pmatrix} \Delta x \\ \Delta y \end{pmatrix} \boldsymbol{\gamma}^T \quad (6.2)$$

With (5.9) and (4.15) one finds

$$\begin{pmatrix} \frac{\partial \mathbf{n}_\gamma^T}{\partial x} \\ \frac{\partial \mathbf{n}_\gamma^T}{\partial y} \end{pmatrix} = \frac{1}{J_0^2} \begin{pmatrix} -J_0 b_1 & (J_1 b_3 - J_2 b_1) & J_0 b_3 \\ J_0 a_1 & (J_2 a_1 - J_1 a_3) & -J_0 a_3 \end{pmatrix} \begin{pmatrix} \xi \\ \xi \eta \\ \eta \end{pmatrix} \boldsymbol{\gamma}^T \quad (6.3)$$

Considering (5.19) and (5.21), the derivatives of the incompatible modes as obtained from (5.36) become

$$\begin{aligned} \frac{\partial \mathbf{w}}{\partial x} &= \frac{2}{J_0^2} \begin{pmatrix} -b_3^2 & a_3 b_3 \\ -b_1^2 & a_1 b_1 \end{pmatrix} \begin{pmatrix} \Delta x \\ \Delta y \end{pmatrix} \\ \frac{\partial \mathbf{w}}{\partial y} &= \frac{2}{J_0^2} \begin{pmatrix} a_3 b_3 & -a_3^2 \\ a_1 b_1 & -a_1^2 \end{pmatrix} \begin{pmatrix} \Delta x \\ \Delta y \end{pmatrix} \end{aligned} \quad (6.4)$$

Again, using (5.9) and (4.15) leads to

$$\begin{aligned} \frac{\partial \mathbf{w}}{\partial x} &= \frac{2}{J_0^2} \begin{pmatrix} -J_0 b_3 & -J_2 b_3 & 0 \\ 0 & J_1 b_1 & J_0 b_1 \end{pmatrix} \begin{pmatrix} \xi \\ \xi \eta \\ \eta \end{pmatrix} \\ \frac{\partial \mathbf{w}}{\partial y} &= \frac{2}{J_0^2} \begin{pmatrix} J_0 a_3 & J_2 a_3 & 0 \\ 0 & -J_1 a_1 & -J_0 a_1 \end{pmatrix} \begin{pmatrix} \xi \\ \xi \eta \\ \eta \end{pmatrix} \end{aligned} \quad (6.5)$$

Corresponding to the first and second-order terms of the Taylor series, the gradient operator  $\mathbf{B}$  is separated into a constant part,  $\mathbf{B}_0$ , and a part  $\mathbf{B}_\ell$ , which is bilinear in  $\xi$  and  $\eta$ :

$$\mathbf{B}^T = \mathbf{B}_0^T + \mathbf{B}_\ell^T \quad (6.6)$$

With (4.5) and (6.1), the constant operator is

$$\mathbf{B}_0^T = \frac{1}{2J_0} \begin{pmatrix} b_3 & -b_1 & 0 & 0 \\ 0 & 0 & -a_3 & a_1 \\ -a_3 & a_1 & b_3 & -b_1 \end{pmatrix} \begin{pmatrix} \mathbf{g}_\xi^T & \mathbf{0} \\ \mathbf{g}_\eta^T & \mathbf{0} \\ \mathbf{0} & \mathbf{g}_\xi^T \\ \mathbf{0} & \mathbf{g}_\eta^T \end{pmatrix} \quad (6.7)$$

The operator

$$\mathbf{B}_\ell^T = \begin{pmatrix} l_1 & 0 \\ 0 & l_2 \\ l_2 & l_1 \end{pmatrix} \begin{pmatrix} \boldsymbol{\gamma}^T & \mathbf{0} \\ \mathbf{0} & \boldsymbol{\gamma}^T \end{pmatrix} = \mathbf{L}^T \boldsymbol{\Gamma}^T \quad (6.8)$$

contains the constant matrix

$$\boldsymbol{\Gamma}^T = \begin{pmatrix} \boldsymbol{\gamma}^T & \mathbf{0} \\ \mathbf{0} & \boldsymbol{\gamma}^T \end{pmatrix} \quad (6.9)$$

with the  $\gamma$ -vector from (5.18), and the matrix

$$\mathbf{L}^T = \begin{pmatrix} l_1 & 0 \\ 0 & l_2 \\ l_2 & l_1 \end{pmatrix} \quad (6.10)$$

with bilinear polynomials as obtained from (6.3):

$$\begin{aligned} l_1 &= -\frac{1}{J_0} \left[ b_1 \xi + \left( \frac{J_2}{J_0} b_1 - \frac{J_1}{J_0} b_3 \right) \xi \eta - b_3 \eta \right] \\ l_2 &= \frac{1}{J_0} \left[ a_1 \xi + \left( \frac{J_2}{J_0} a_1 - \frac{J_1}{J_0} a_3 \right) \xi \eta - a_3 \eta \right] \end{aligned} \quad (6.11)$$

According to (4.5), the operator  $\mathbf{G}$  is derived from (6.5) as

$$\mathbf{G}^T = \begin{pmatrix} g_1 & g_2 & 0 & 0 \\ 0 & 0 & g_3 & g_4 \\ g_3 & g_4 & g_1 & g_2 \end{pmatrix} \quad (6.12)$$

with the polynomials

$$\begin{aligned} g_1 &= -\frac{2}{J_0} b_3 \left[ \xi + \frac{J_2}{J_0} \xi \eta \right] & g_3 &= \frac{2}{J_0} a_3 \left[ \xi + \frac{J_2}{J_0} \xi \eta \right] \\ g_2 &= \frac{2}{J_0} b_1 \left[ \eta + \frac{J_1}{J_0} \xi \eta \right] & g_4 &= -\frac{2}{J_0} a_1 \left[ \eta + \frac{J_1}{J_0} \xi \eta \right] \end{aligned} \quad (6.13)$$

Now, the gradient operators  $\mathbf{B}$  and  $\mathbf{G}$  are defined completely. Prior to forming the element stiffness matrix, an analysis is carried out on the method of integration.

## 7. INTEGRATION

First, simple integration formulae are given:

$$\int_{-1}^1 \int_{-1}^1 \xi d\xi d\eta = 0 \quad \int_{-1}^1 \int_{-1}^1 \xi \eta d\xi d\eta = 0 \quad \int_{-1}^1 \int_{-1}^1 \eta d\xi d\eta = 0 \quad (7.1)$$

To form an element stiffness matrix, functions  $f$  are integrated over a quadratic element in the master element space. The rule for the change of variables is

$$\int f(x, y) dV = \int_{-1}^1 \int_{-1}^1 f(\xi, \eta) J d\xi d\eta \quad (7.2)$$

with the determinant of the Jacobian

$$J(\xi, \eta) = J_0 + J_1 \xi + J_2 \eta \quad (4.14)$$

According to the mean value theorem of integrals, within the region of integration there is a point with the co-ordinates  $(\bar{\xi}, \bar{\eta})$  such that

$$\int_{-1}^1 \int_{-1}^1 f(\xi, \eta) J(\xi, \eta) d\xi d\eta = J(\bar{\xi}, \bar{\eta}) \int_{-1}^1 \int_{-1}^1 f(\xi, \eta) d\xi d\eta \quad (7.3)$$

For constant and for even functions  $f$ , the integration over the left-hand side of (7.3) is zero for those terms containing  $J_1 \xi$  and  $J_2 \eta$ . Consequently, for such functions, the co-ordinates  $(\bar{\xi}, \bar{\eta}) = (0, 0)$  satisfy (7.3) identically. For other functions  $f$ , the choice of  $(\bar{\xi}, \bar{\eta}) = (0, 0)$  provides for an approximation, which shall be used, and which has to be used for the proposed element formulation in order to maintain convergence with mesh refinement. Equivalent to that approach is the use of a modified change of variables in which the determinant of the Jacobian is evaluated at the element centre:

$$\int f(x, y) dV = \int_{-1}^1 \int_{-1}^1 f(\xi, \eta) J_0 d\xi d\eta \quad (7.4)$$

With (3.2), (6.6), (6.12) and (7.4), the element stiffness matrix can now be obtained from static condensation as described in (3.9). A more efficient procedure is possible. It is presented subsequently.

For a linear elastic material, the matrix of material stiffnesses,  $\mathbf{E}$ , is constant throughout the element. Therefore, all integrations of terms containing the constant gradient operator,  $\mathbf{B}_0$ , and a linear operator,  $\mathbf{B}_\ell$  or  $\mathbf{G}$ , yield zero:

$$\begin{aligned} \int \mathbf{B}_0 \mathbf{E} \mathbf{B}_\ell^T dV &= \mathbf{0} & \int \mathbf{B}_\ell \mathbf{E} \mathbf{B}_0^T dV &= \mathbf{0} \\ \int \mathbf{B}_0 \mathbf{E} \mathbf{G}^T dV &= \mathbf{0} & \int \mathbf{G} \mathbf{E} \mathbf{B}_0^T dV &= \mathbf{0} \end{aligned} \quad (7.5)$$

This is because the integrations in (7.5) include terms only being linear or bilinear in  $\xi$  and  $\eta$ . In the case of a linear elastic material, the operators are said to be uncoupled, which is the essential property to provide for convergence with mesh refinement.

Since the gradient operators involved are either constant or bilinear, all integrations may be carried out analytically. Explicit solutions are not presented here. In contrast, for most element formulations, numerical integration is inevitable due to rational functions involving  $1/J$ , where  $J$  is a function of  $\xi$  and  $\eta$ .

## 8. EQUILIBRIUM

To obtain the relation  $\boldsymbol{\phi} = \boldsymbol{\phi}(\mathbf{d})$ , the constraint equation

$$\left( \int \mathbf{G} \mathbf{E} \mathbf{B}^T dV \right) \mathbf{d} + \left( \int \mathbf{G} \mathbf{E} \mathbf{G}^T dV \right) \boldsymbol{\phi} = \mathbf{0} \quad (3.6)$$

is evaluated. Corresponding to (6.6), the operator  $\mathbf{B}$  is expressed in terms of  $\mathbf{B}_0$  and  $\mathbf{B}_\ell$ . Then with (6.8) and (7.5), the first term on the left-hand side of (3.6) becomes

$$\left( \int \mathbf{G} \mathbf{E} \mathbf{B}^T dV \right) \mathbf{d} = \left( \int \mathbf{G} \mathbf{E} \mathbf{L}^T dV \right) \boldsymbol{\Gamma}^T \mathbf{d} \quad (8.1)$$

Evaluation of the integral on the right-hand side of (8.1) leads to a  $(4 \times 2)$  matrix with column vectors  $\mathbf{t}_u$  and  $\mathbf{t}_v$ :

$$(\mathbf{t}_u \quad \mathbf{t}_v) = \int \mathbf{G} \mathbf{E} \mathbf{L}^T dV \quad (8.2)$$

Using (4.1) and (6.9), the remaining term on the right-hand side of (8.1) is written as

$$\boldsymbol{\Gamma}^T \mathbf{d} = \begin{pmatrix} \boldsymbol{\gamma}^T & \mathbf{0} \\ \mathbf{0} & \boldsymbol{\gamma}^T \end{pmatrix} \begin{pmatrix} \mathbf{u} \\ \mathbf{v} \end{pmatrix} = \begin{pmatrix} \boldsymbol{\gamma}^T \mathbf{u} \\ \boldsymbol{\gamma}^T \mathbf{v} \end{pmatrix} \quad (8.3)$$

Therefore, the vector  $\Phi$  in (3.6) is assumed to be of the form

$$\Phi = (\Phi_u \quad \Phi_v) \begin{pmatrix} \boldsymbol{\gamma}^T \mathbf{u} \\ \boldsymbol{\gamma}^T \mathbf{v} \end{pmatrix} = \Phi \boldsymbol{\Gamma}^T \mathbf{d} \quad (8.4)$$

Now, to calculate  $\Phi(\mathbf{d})$ , the two columns  $\Phi_u$  and  $\Phi_v$  of the  $(4 \times 2)$  matrix

$$\Phi = (\Phi_u \quad \Phi_v) \quad (8.5)$$

must be found. The second integral in (3.6) leads to a symmetric, positive-definite  $(4 \times 4)$  matrix

$$\mathbf{H} = \int \mathbf{G} \mathbf{E} \mathbf{G}^T dV \quad (8.6)$$

Introducing (8.2) and (8.3) into (8.1), then introducing (8.1), (8.4) and (8.6) into (3.6) generates an equivalent expression for the equilibrium constraint (3.6):

$$(\mathbf{t}_u \quad \mathbf{t}_v) \begin{pmatrix} \boldsymbol{\gamma}^T \mathbf{u} \\ \boldsymbol{\gamma}^T \mathbf{v} \end{pmatrix} + \mathbf{H} (\Phi_u \quad \Phi_v) \begin{pmatrix} \boldsymbol{\gamma}^T \mathbf{u} \\ \boldsymbol{\gamma}^T \mathbf{v} \end{pmatrix} = \mathbf{0} \quad (8.7)$$

Finally, from (8.7), the form

$$(\mathbf{t}_u + \mathbf{H} \Phi_u) \boldsymbol{\gamma}^T \mathbf{u} + (\mathbf{t}_v + \mathbf{H} \Phi_v) \boldsymbol{\gamma}^T \mathbf{v} = \mathbf{0} \quad (8.8)$$

is obtained, which must hold for all displacements  $\mathbf{u}$  and  $\mathbf{v}$ . Therefore, expressions for  $\Phi_u$  and  $\Phi_v$  are obtained from (8.8) by solving the two equations

$$\mathbf{H} \Phi_u = -\mathbf{t}_u \quad \mathbf{H} \Phi_v = -\mathbf{t}_v \quad (8.9)$$

on the element level. Then (8.4) is equivalent to  $\Phi = \Phi(\mathbf{d})$  in (3.7).

## 9. ELEMENT STIFFNESS MATRIX

For the calculation of the element stiffness matrix, a complete gradient operator is formed using the results obtained from the evaluation of the equilibrium constraint.

With (6.6), (6.8) and (8.4), the expression for the strain field in (3.10) takes the form

$$\boldsymbol{\epsilon} = \mathbf{B}_0^T \mathbf{d} + \mathbf{L}^T \boldsymbol{\Gamma}^T \mathbf{d} + \mathbf{G}^T \Phi \boldsymbol{\Gamma}^T \mathbf{d} = (\mathbf{B}_0^T + \mathbf{B}_*^T) \mathbf{d} = \bar{\mathbf{B}}^T \mathbf{d} \quad (9.1)$$

Once a global solution for the displacements,  $\mathbf{d}$ , is available, (9.1) may be used to evaluate the element stress field by means of the constitutive equation (3.1). Through (9.1), the gradient operator

$$\mathbf{B}_*^T = (\mathbf{L}^T + \mathbf{G}^T \Phi) \boldsymbol{\Gamma}^T \quad (9.2)$$

is defined. The matrices  $\mathbf{L}$  and  $\mathbf{G}$  are bilinear in  $\xi$  and  $\eta$ , the matrices  $\Phi$  and  $\boldsymbol{\Gamma}$  are constant. Therefore, the matrix  $\mathbf{B}_*$  is bilinear too. Consequently, the operators  $\mathbf{B}_0$  and  $\mathbf{B}_*$  are

uncoupled as well:

$$\int \mathbf{B}_0 \mathbf{E} \mathbf{B}_0^T dV = \mathbf{0} \quad \int \mathbf{B}_* \mathbf{E} \mathbf{B}_0^T dV = \mathbf{0} \quad (9.3)$$

Then the element stiffness matrix in (3.11) becomes

$$\mathbf{K} = \mathbf{K}_0 + \mathbf{K}_* = \int \mathbf{B}_0 \mathbf{E} \mathbf{B}_0^T dV + \int \mathbf{B}_* \mathbf{E} \mathbf{B}_*^T dV \quad (9.4)$$

The integration of  $\mathbf{K}_0$  includes only constants. The result is

$$\mathbf{K}_0 = 4J_0 \mathbf{B}_0 \mathbf{E} \mathbf{B}_0^T \quad (9.5)$$

which is the same matrix as obtained when performing a 1-point Gauss quadrature on the standard isoparametric element. With (9.2), the second matrix in (9.4) becomes

$$\mathbf{K}_* = \Gamma \left[ \int (\mathbf{L} + \Phi^T \mathbf{G}) \mathbf{E} (\mathbf{L}^T + \mathbf{G}^T \Phi) dV \right] \Gamma^T \quad (9.6)$$

The integration in (9.6) yields a symmetric  $(2 \times 2)$  matrix which contains the coefficients for the element stabilization:

$$\begin{pmatrix} \varepsilon_1 & \varepsilon_2 \\ \varepsilon_2 & \varepsilon_3 \end{pmatrix} = \int (\mathbf{L} + \Phi^T \mathbf{G}) \mathbf{E} (\mathbf{L}^T + \mathbf{G}^T \Phi) dV \quad (9.7)$$

Then with (6.9), the stabilization matrix<sup>8, 9, 18</sup> is

$$\mathbf{K}_* = \begin{pmatrix} \varepsilon_1 \gamma \gamma^T & \varepsilon_2 \gamma \gamma^T \\ \varepsilon_2 \gamma \gamma^T & \varepsilon_3 \gamma \gamma^T \end{pmatrix} \quad (9.8)$$

For the special case of a rectangular element geometry,  $\mathbf{K}_*$  reduces to the stabilization matrix derived previously.<sup>24</sup>

Table I. Summary of element formulation

Term	Dimension	Equation	Description
$\mathbf{E}$	$(3 \times 3)$	(3.2)	Input data material
$\mathbf{x}, \mathbf{y}$	$(4 \times 1)$	(4.8)	Input data co-ordinates
$\mathbf{g}_x, \mathbf{g}_y, \mathbf{h}$	$(4 \times 1)$	(4.7)	Definitions
$a_1 \dots b_3$	Scalars	(4.9)	Constants
$J_0, J_1, J_2$	Scalars	(4.15)	Constants
$\mathbf{B}_0$	$(8 \times 3)$	(6.7)	Constant gradient operator
$\mathbf{K}_0$	$(8 \times 8)$	(9.5)	Constant gradient matrix
$\mathbf{L}$	$(2 \times 3)$	(6.10)	Part of gradient operator
$\mathbf{G}$	$(4 \times 3)$	(6.12)	Gradient operator
$\int dV$	—	(7.4)	Change of variables
$\mathbf{t}_u, \mathbf{t}_v$	$(4 \times 1)$	(8.2)	Integration
$\mathbf{H}$	$(4 \times 4)$	(8.6)	Integration
$\Phi$	$(4 \times 2)$	(8.5)	Solution of (8.9)
$\varepsilon_1, \varepsilon_2, \varepsilon_3$	Scalars	(9.7)	Integration
$\gamma$	$(4 \times 1)$	(5.18)	Constant
$\mathbf{K}_*$	$(8 \times 8)$	(9.8)	Stabilization matrix
$\mathbf{K}$	$(8 \times 8)$	(9.4)	Element stiffness matrix
$\boldsymbol{\varepsilon}$	$(3 \times 1)$	(9.1)	Element strains, with (6.9)
$\boldsymbol{\sigma}$	$(3 \times 1)$	(3.1)	Element stresses

## 10. SUMMARY

The formulation for the proposed element consists of three major steps: First, expressions for gradient operators are obtained from a Taylor series expansion of the element basis functions. Second, the equilibrium constraint is evaluated on the element level. Third, the element stiffness matrix is calculated. A complete summary of the element formulation is given in Table I.

## 11. NUMERICAL EXAMPLES

For a comparison of numerical performances, the following elements are chosen:

- Q4 - isoparametric Taig element with  $(2 \times 2)$  Gauss quadrature<sup>25</sup>
- QM6 - incompatible Taylor element,<sup>30</sup> equivalent to the assumed strain element of Simo and Rifai<sup>32</sup>
- $5\beta$ -I - assumed stress Pian-Sumihara element<sup>35</sup>
- $5\beta$ -A - assumed stress element of Yuan *et al.*<sup>39, 56</sup>
- $5\beta$ -NT - assumed stress element of Di and Ramm<sup>40, 57</sup>
- QS6 - present formulation

Here, reference is given to the sources of the presented numerical data. Further, for the analysis, the finite element program FEAP is used.<sup>37, 58</sup>

Besides the unmodified quadrilateral, Q4, the selection is of formulations with highest numerical accuracy known to date.

Standard model problems are chosen. Numerical results are given in terms of errors with respect to analytical solutions. In the literature, most of the results are presented in absolute numbers. Therefore, corresponding data for standard reference solutions are given as well.

The material parameters

$$\bar{E} = \frac{E_1^2 - E_2^2}{E_1} \quad \bar{\nu} = \frac{E_2}{E_1} \quad (11.1)$$

are introduced to describe the analytical solutions. With (3.3) and (3.4), for plane stress,

$$\bar{E} = E \quad \bar{\nu} = \nu \quad (11.2)$$

whereas for plane strain,

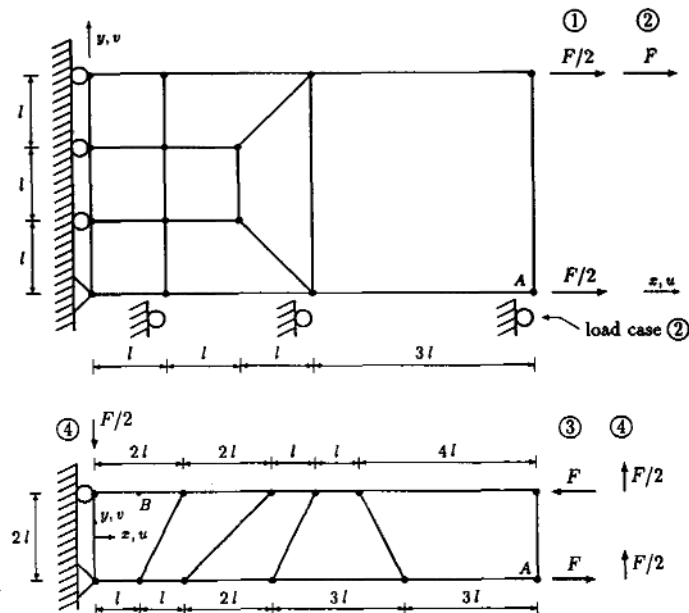
$$\bar{E} = \frac{E}{1 - \nu^2} \quad \bar{\nu} = \frac{\nu}{1 - \nu} \quad (11.3)$$

All model problems are calculated in the state of plane stress. In a related work,<sup>59</sup> numerical results are presented for the incompressible limit in plane strain.

In Figure 3, load case ① provides a test for the correct representation of a state of constant stress and strain. The analytical solutions for the displacements are

$$u = \frac{F}{3\bar{E}} \frac{x}{l} \quad v = -\bar{\nu} \frac{F}{3\bar{E}} \frac{y}{l} \quad (11.4)$$

where the load  $F$  is of dimension (force/length). Numerical results are given in Table II. All elements pass this patch test and yield the exact analytical solution.

Figure 3. Cantilevers subject to tension, moment and shear<sup>25,30</sup>

Load case ② in Figure 3 describes the upper-half of a cantilever beam subject to a moment tip load. To provide for symmetry, the nodes on the lower edge are constrained in the  $x$ -direction. The analytical solutions are

$$u = \frac{F}{3\bar{E}} \frac{xy}{l^2} \quad v = -\frac{F}{6\bar{E}} \left\{ \left( \frac{x}{l} \right)^2 + \bar{v} \left( \frac{y}{l} \right)^2 \right\} \quad (11.5)$$

In Table II, results are given for the vertical displacement of node A. All elements perform similarly. Only the Q4 exhibits a somewhat lower accuracy.

For the cantilever in load case ③, the analytical solutions for the displacements are

$$u = -\frac{3F}{\bar{E}} \frac{xy}{l^2} \quad v = \frac{3F}{2\bar{E}} \left\{ \left( \frac{x}{l} \right)^2 + \bar{v} \left[ \left( \frac{y}{l} \right)^2 - 1 \right] \right\} \quad (11.6)$$

Table II. Numerical results for cantilever model problems

Error (%)	①		②		③		④	
	$u_A$	$v_A$	$v_A$	$\sigma_{xB}$	$v_A$	$\sigma_{xB}$	$v_A$	$\sigma_{xB}$
Q4	0.0	-5.56	-54.30	-41.30	-50.41	-39.56		
QM6	0.0	-2.17	-4.00	-16.30	-4.01	-15.01		
$5\beta$ -I	0.0	-2.00	-3.82	0.47	-3.92	2.15		
$5\beta$ -A	0.0	—	-3.51	0.43	-3.75	2.16		
$5\beta$ -NT	0.0	-2.11	-3.77	-0.57	-3.80	1.11		
QS6	0.0	-2.11	-0.28	11.63	-0.27	13.60		

As compared to (11.5), the additional term in  $v$  reflects the non-symmetric boundary conditions. The analytical solution for the stress field is

$$\sigma_x = -\frac{3Fy}{l^2} \quad (11.7)$$

Almost the exact solution for the vertical tip displacement of node  $A$  is obtained from the QS6 formulation. The assumed stress elements as well as the QM6 yield a slightly larger error. Here and for subsequent model problems, the accuracy of the Q4 element is low.

All assumed stress elements provide good results in the stresses at point  $B$ , while the error for the elements QS6 and QM6 is higher. Stresses may be evaluated at other points of the beam. Then the numerical error obtained from assumed stress formulations is of the order of magnitude being obtained from the element proposed here.<sup>60</sup>

Load case ④ in Figure 3 describes a cantilever beam subject to a parabolically varying end shear load.<sup>61</sup> For a fixed root section, the analytical solutions are<sup>62</sup>

$$\tilde{u} = -\frac{Fy}{6EI} \left\{ (6L - 3x)x + (2 + \bar{v}) \left[ y^2 - \left( \frac{H}{2} \right)^2 \right] \right\} \quad (11.8)$$

$$\tilde{v} = \frac{F}{6EI} \left\{ 3\bar{v}y^2(L - x) + (4 + 5\bar{v}) \left( \frac{H}{2} \right)^2 x + \left( L - \frac{x}{3} \right) 3x^2 \right\} \quad (11.9)$$

with

$$L = 10l \quad H = 2l \quad I = \frac{H^3}{12} \quad (11.10)$$

Due to the unsymmetric boundary conditions, the reference solutions for the numerical analysis become

$$u = \tilde{u} \quad v = \tilde{v} - \tilde{v}(x = 0, y = -H/2) \quad (11.11)$$

Stresses  $\sigma_x$  are described by

$$\sigma_x = -\frac{Fy}{I}(L - x) \quad (11.12)$$

For load case ④, the errors in the numerical solutions are similar to those obtained for load case ③.

Table III gives parameters and corresponding reference solutions used in the literature for the model problems in Figure 3.

Table III. Parameters and reference solutions

	①	②	③	④
$E$	1	1	1500	1500
$v$	0.25	0.25	0.25	0.25
$F$	3	3	1000	300
$l$	1	1	1	1
$u_A$	6.0	—	—	—
$v_A$	—	-18.0	100.0	102.2
$\sigma_{xB}$	—	—	-3000	-4050

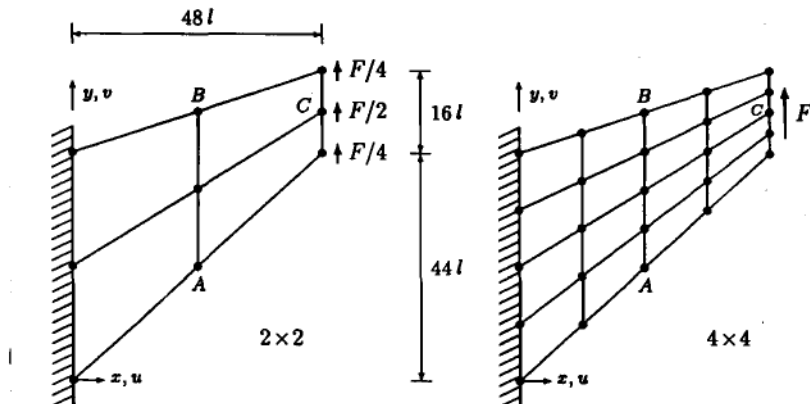


Figure 4. Beam subject to end shear load

Known as Cook's<sup>25</sup> membrane problem, Figure 4 shows a beam under a uniformly distributed end shear load. An analytical solution does not exist for this model problem. Therefore, the beam is modelled with a mesh of  $128 \times 128$  elements to obtain a reference solution. Using the parameters

$$E = 1 \quad v = \frac{1}{3} \quad F = 1 \quad l = 1$$

the  $5\beta$ -I element and the QS6 element both yield the same numerical answers

$$v_c = 23.96 \quad \sigma_{\max A} = 0.2369 \quad \sigma_{\min B} = -0.2035$$

for the vertical displacement of node C and for the maximum and minimum principal stresses at the nodes A and B, respectively. Numerical results are presented in Table IV. Now, for solutions in stresses, the QS6 exhibits a similar accuracy as the assumed stress elements.

For stress calculations, it should be distinguished between the direct evaluation of element stresses, as performed in load cases ③ and ④ of Figure 3, and the calculation of stress averages obtained from adjacent elements, as performed for the model problem in Figure 4. The latter is of more practical importance since a continuous stress field can only be described by means of a stress smoothing procedure. In such application, as for the problem in Figure 4, the high quality of the QS6 for stress calculations is indicated by the results shown in Table IV.

A convergence study is carried out as well using the beam in Figure 4. The mesh is subdivided regularly using  $2 \times 2 \dots 64 \times 64$  elements. On logarithmic scales, Figure 5 shows solutions for the

Table IV. Numerical results for beam subject to end shear load

Error (%)	2 × 2			4 × 4		
	$v_c$	$\sigma_{\max A}$	$\sigma_{\min B}$	$v_c$	$\sigma_{\max A}$	$\sigma_{\min B}$
Q4	-50.54	-45.93	-54.99	-23.62	-19.59	-25.80
QM6	-12.15	-19.80	-23.10	-3.92	-5.49	-8.94
$5\beta$ -I	-11.81	-21.74	-23.83	-3.92	-5.41	-8.80
$5\beta$ -A	-10.89	-17.43	-28.85	-3.84	-4.56	-8.65
$5\beta$ -NT	-10.39	-27.27	-12.43	-3.80	-6.50	-9.73
QS6	-12.10	-17.10	-28.01	-3.92	-4.48	-8.35

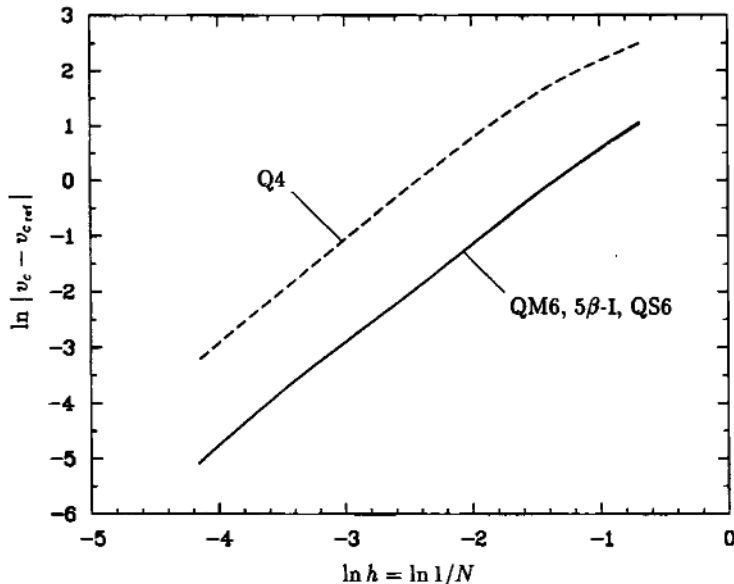


Figure 5. Convergence with mesh refinement for linear elastic material

error in tip displacement,  $|v_c - v_{c,ref}|$ , over a characteristic element length  $h$ , obtained from the number of elements per side,  $N$ . For the formulations analysed, the rate of convergence is identical. Only the difference in accuracy as compared to the Q4 becomes evident.

Being introduced by Pian and Sumihara,<sup>35</sup> a rigorous test problem is shown in Figure 6, for which the analytical solution is given in (11.6). The error of the vertical tip deflection at node  $A$  is calculated for an increasing mesh distortion,  $a$ . Results are presented in Figure 7.

For rectangles, all elements but the Q4 yield the exact solution. The elements QM6, 5 $\beta$ -I, 5 $\beta$ -A and QS6, all provide for a similar sensitivity to mesh distortion.\*

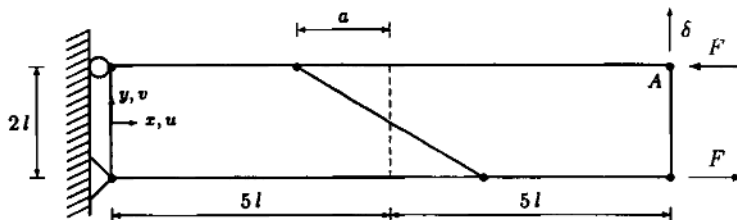


Figure 6. Cantilever subject to moment tip load

\* It appears that the element 5 $\beta$ -NT yields superior results as compared to the other elements.<sup>40</sup> But, a study on the lower tip node exhibits an error of up to +60 per cent for that element.<sup>57</sup> This is in contrast to the other formulations, where just slightly improved solutions are obtained for the lower node.

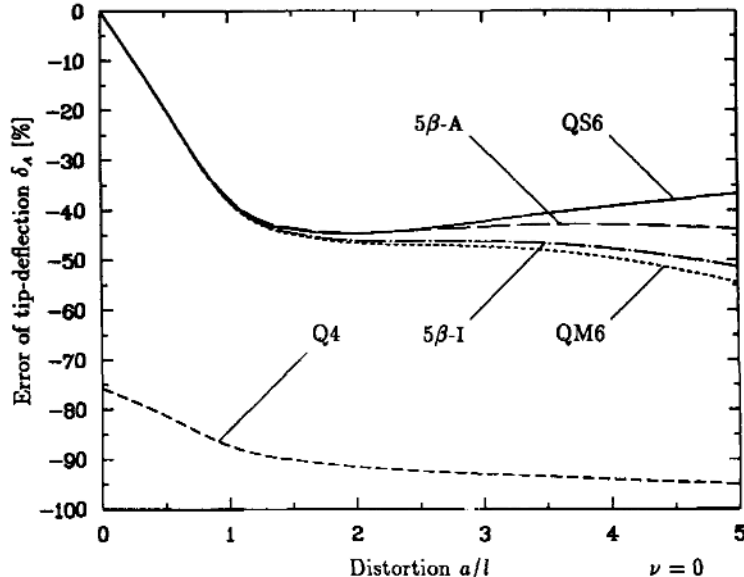


Figure 7. Element test on sensitivity to geometric distortion

## 12. INELASTIC MATERIAL

Within the framework of the proposed element formulation, an application is given for the analysis of inelastic materials. Geometrically linear and rate-independent elastoplastic problems are considered.

To begin, the non-linear equations for the finite element approximation are summarized. Next, their solution using the Newton procedure is outlined. Similarities and differences to the assumed strain approach of Simo and Rifai<sup>32</sup> are discussed. Finally, an elastoplastic model problem is calculated, and the results are compared with existing approaches.

### 12.1. Non-linear equations

The constitutive equations for a rate-independent elastoplastic material are summarized as follows.<sup>63</sup>

$$\begin{aligned} \boldsymbol{\varepsilon}^e &= \boldsymbol{\varepsilon} - \boldsymbol{\varepsilon}^p & \boldsymbol{\sigma} &= \mathbf{E} \boldsymbol{\varepsilon}^e \\ \dot{\boldsymbol{\varepsilon}}^p &= \lambda \frac{\partial f}{\partial \boldsymbol{\sigma}} & \dot{q} &= \lambda \frac{\partial f}{\partial q} \\ f(\boldsymbol{\sigma}, \alpha) &\leq 0 & \lambda &\geq 0 & \lambda f &= 0 \end{aligned} \quad (12.1)$$

Here,  $\boldsymbol{\varepsilon}^e$  and  $\boldsymbol{\varepsilon}^p$  denote the elastic and the plastic strains, respectively. Equation (12.1)<sub>2</sub> represents the elasticity law. The flow rule for the plastic strains is given in (12.1)<sub>3</sub>, and (12.1)<sub>4</sub> denotes the isotropic hardening law with the isotropic hardening variable  $q$ . The yield condition,  $f \leq 0$ , depends on the stresses, and for an isotropic hardening material, on the equivalent plastic strain  $\alpha$  as well. The material model represents a history-dependent response, such that a time integration is needed. A standard solution procedure is given by the return-mapping algorithm. It

is derived by application of the Euler backward integration rule for the evaluation of all time-dependent quantities.<sup>58, 63</sup> The solution of (12.1) leads to an expression for the elastoplastic stresses  $\sigma_k$  at time  $t_k$ . From these, the associated constitutive tangent matrix  $E_k^t$  can be computed:<sup>64</sup>

$$\sigma_k = \sigma_k^{tr} - \lambda_k n_k \quad E_k^t = \frac{\partial \sigma_k}{\partial \varepsilon_k} \quad (12.2)$$

In (12.2),  $\sigma_k^{tr}$  is the so-called trial stress, representing the pure elastic response. If the trial stress lies outside the yield surface, then  $\lambda_k$  measures the distance from the trial stress point to the yield surface. The parameter  $\lambda_k$  is obtained from the consistency conditions (12.1)<sub>5-7</sub>, and  $n_k$  represents the direction of the return map onto the yield surface.

Within the finite element formulation, the strain field  $\varepsilon$  is described by the linear form (2.2). Then the elastoplastic stresses  $\sigma_k$  are obtained for time  $t_k$  from the solution of (12.1) and (12.2).

Corresponding to (2.6) and (2.7), the weak form of equilibrium for the deformable body leads to the equations for the finite element approximation

$$\begin{aligned} \Psi^B(d_k, \phi_k) &= f - \int B \sigma_k dV = 0 \\ \Psi^G(d_k, \phi_k) &= - \int G \sigma_k dV = 0 \end{aligned} \quad (12.3)$$

where  $\Psi^B$  and  $\Psi^G$  denote residuals.

## 12.2. Newton procedure

As outlined by Simo and Rifai,<sup>32</sup> the finite element solution of the non-linear equations (12.3) is obtained by a Newton procedure.

The residuals in (12.3) are approximated by first-order Taylor series expansions of the form

$$\Psi_{k+1}(d_k + \Delta d_k, \phi_k + \Delta \phi_k) \cong \Psi_k(d_k, \phi_k) + \frac{\partial \Psi_k}{\partial d_k} \Delta d_k + \frac{\partial \Psi_k}{\partial \phi_k} \Delta \phi_k = 0 \quad (12.4)$$

Using (2.2) and (12.2), the differentiation of the element stresses  $\sigma$  with respect to  $d$  and  $\phi$  yields

$$\begin{aligned} \frac{\partial \sigma_k}{\partial d_k} &= \frac{\partial \sigma_k}{\partial \varepsilon_k} \frac{\partial \varepsilon_k}{\partial d_k} = E_k^t B^T \\ \frac{\partial \sigma_k}{\partial \phi_k} &= \frac{\partial \sigma_k}{\partial \varepsilon_k} \frac{\partial \varepsilon_k}{\partial \phi_k} = E_k^t G^T \end{aligned} \quad (12.5)$$

Introduction of (12.5) via (12.4) into (12.3) leads to the system of equations

$$\begin{aligned} \left( \int B E_k^t B^T dV \right) \Delta d_k + \left( \int B E_k^t G^T dV \right) \Delta \phi_k &= f - \int B \sigma_k dV \\ \left( \int G E_k^t B^T dV \right) \Delta d_k + \left( \int G E_k^t G^T dV \right) \Delta \phi_k &= - \int G \sigma_k dV \end{aligned} \quad (12.6)$$

From these, the Newton procedure is obtained as follows:

Starting at  $\mathbf{f} = \mathbf{0}$ , the external loads are increased stepwise up to their final value. The initial values for the displacements and for the internal element degrees of freedom are  $\mathbf{d}_0 = \mathbf{0}$  and  $\boldsymbol{\phi}_0 = \mathbf{0}$ , respectively. As the residuals  $\Psi^B$  and  $\Psi^G$  become sufficiently small within the iteration for a single load step, the Newton procedure yields new values for  $\mathbf{d}$  and  $\boldsymbol{\phi}$ . These are the initial values for the next load step. The last load step then leads to the final solution for the displacements.

Within a Newton iteration, from  $\mathbf{d}_k$  and  $\boldsymbol{\phi}_k$ , the strains

$$\boldsymbol{\epsilon}_k = \mathbf{B}^T \mathbf{d}_k + \mathbf{G}^T \boldsymbol{\phi}_k \quad (12.7)$$

are evaluated. Then the stresses  $\boldsymbol{\sigma}_k$  and the tangent operator  $\mathbf{E}_k^t$  are obtained from (12.1) and (12.2). According to (12.6), the matrices

$$\mathbf{K}_k = \int \mathbf{B} \mathbf{E}_k^t \mathbf{B}^T dV \quad \mathbf{T}_k = \int \mathbf{B} \mathbf{E}_k^t \mathbf{G}^T dV \quad \mathbf{H}_k = \int \mathbf{G} \mathbf{E}_k^t \mathbf{G}^T dV \quad (12.8)$$

as well as the vectors

$$\Psi_k^B = \mathbf{f} - \int \mathbf{B} \boldsymbol{\sigma}_k dV \quad \Psi_k^G = - \int \mathbf{G} \boldsymbol{\sigma}_k dV \quad (12.9)$$

are calculated. Here, the gradient operator  $\mathbf{B} = \mathbf{B}_0 + \mathbf{B}_t$  is defined by (6.7) and (6.8), the operator  $\mathbf{G}$  is defined by (6.12).

From (12.7),  $\boldsymbol{\sigma}_k$  and  $\mathbf{E}_k^t$  are calculated separately for each Gauss quadrature point. Therefore,  $\mathbf{E}_k^t$  is not constant throughout an element. Consequently, the gradient operators are no longer uncoupled, which is in contrast to the linear elastic case. Thus, for inelastic analysis, the proposed formulation of underintegration and stabilization may not be used to generate the element stiffness matrix.

Elimination of  $\Delta\boldsymbol{\phi}_k$  in (12.6) yields the system of equations

$$\bar{\mathbf{K}}_k \Delta\mathbf{d}_k = \bar{\Psi}_k \quad (12.10)$$

with the tangent stiffness matrix

$$\bar{\mathbf{K}}_k = \mathbf{K}_k - \mathbf{T}_k \mathbf{H}_k^{-1} \mathbf{T}_k^T \quad (12.11)$$

and the residual

$$\bar{\Psi}_k = \Psi_k^B - \mathbf{T}_k \mathbf{H}_k^{-1} \Psi_k^G \quad (12.12)$$

From (12.10), the global solution for  $\Delta\mathbf{d}_k$  leads to the displacements

$$\mathbf{d}_{k+1} = \mathbf{d}_k + \Delta\mathbf{d}_k \quad (12.13)$$

On the element level, the internal degrees of freedom for the iteration  $k + 1$  are obtained through

$$\boldsymbol{\phi}_{k+1} = \boldsymbol{\phi}_k + \mathbf{H}_k^{-1} \Psi_k^G - \mathbf{H}_k^{-1} \mathbf{T}_k^T \Delta\mathbf{d}_k \quad (12.14)$$

Therefore, from the previous iteration, the results for  $\boldsymbol{\phi}_k + \mathbf{H}_k^{-1} \Psi_k^G$  and  $\mathbf{H}_k^{-1} \mathbf{T}_k^T$  must be stored on the element level.

With (12.13) and (12.14), the next iteration is started via (12.7). Once  $\Delta\mathbf{d}_k$  and  $\bar{\Psi}_k$  are sufficiently small, the Newton iteration for the load step is completed.

Near the solution  $\bar{\Psi}_{k+1} = \mathbf{0}$ , the rate of convergence for the Newton procedure is of second order.

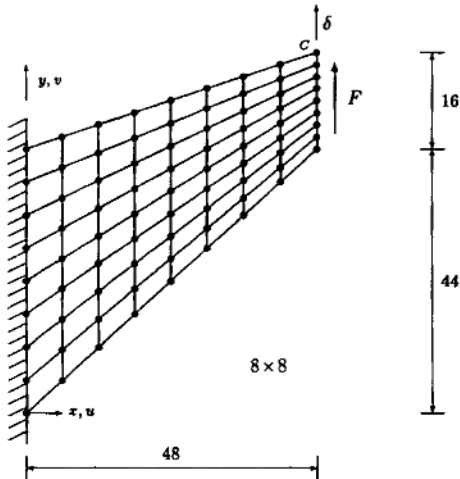


Figure 8. Beam for elastoplastic analysis

### 12.3. Comparison with assumed strain formulation

For the analysis of inelastic materials, the assumed strain approach of Simo and Rifai<sup>32</sup> is based on the 3-field Hu-Washizu variational principle. The equations derived for the finite element approximation are equivalent to those given in (2.6), (2.7) and (12.3). Here, (2.7) is the counterpart to the constraint equation on the enhanced strain field.<sup>24, 65</sup>

An enhanced strain formulation for the analysis of geometrically non-linear problems is given by Simo and Armero.<sup>33</sup> Similarly, the present element formulation can be extended to include problems of large deformations.<sup>66</sup>

The main difference between the present approach and the assumed strain concept is due to the choice of the gradient operators  $\mathbf{B}$  and  $\mathbf{G}$ . For the assumed strain quadrilateral, these operators contain rational function with terms  $1/J$  and  $J_0/J$ . But, in the case of a distorted element geometry, the determinant of the Jacobian in (4.14),  $J$ , may become zero or negative at a Gauss quadrature point. Therefore, the robustness of the assumed strain quadrilateral may be limited.

In the present formulation, the operators  $\mathbf{B}$  and  $\mathbf{G}$  contain only linear functions. Instead of  $J$ ,  $J_0$  appears in the denominator. The latter is proportional to the element area,  $A$ :

$$A = \int_{-1}^1 \int_{-1}^1 J d\xi d\eta = 4J_0 \quad (12.15)$$

Consequently, with respect to geometric distortion, the QS6 element appears to be robust.

### 12.4. Numerical example

For the elastoplastic analysis, the elements Q4, QM6 and QS6 are compared. The formulation for the QM6 is equivalent to the assumed strain approach of Simo and Rifai.<sup>32</sup>

A beam subject to a uniformly distributed end shear load is used as a model problem,<sup>32</sup> and is shown in Figure 8. The vertical displacement  $\delta$  of the upper tip node C is calculated. A regular mesh refinement is carried out, using  $2 \times 2 \dots 64 \times 64$  elements. Through 18 load steps, the tip

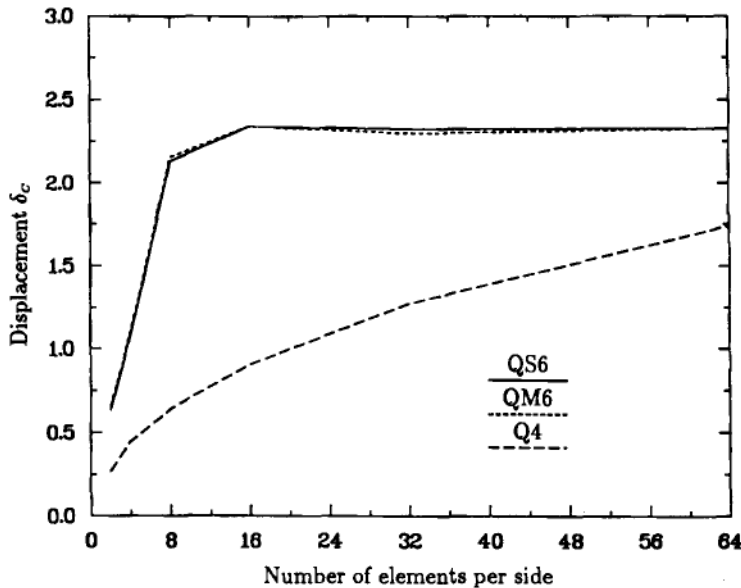


Figure 9. Convergence with mesh refinement for elastoplasticity

load  $F$  is increased up to its final value:

$$F = 0 \dots 1.8 \quad \Delta F = 0.1$$

For the elastoplastic analysis in plane strain, the von Mises flow rule is used in conjunction with linear isotropic hardening. The numerical implementation of the constitutive equation is described by Zienkiewicz and Taylor<sup>58</sup> as well as by Simo and Hughes.<sup>63</sup>

The values for Young's Modulus  $E$ , Poisson's ratio  $\nu$ , the yield stress  $\sigma_Y$  and the isotropic hardening parameter  $H$  are

$$E = 70 \quad \nu = \frac{1}{3} \quad \sigma_Y = 0.243 \quad H = 0.135$$

In Figure 9 results for displacements  $\delta_c$  are given over the number of elements per side. The accuracy of the elements QM6 and QS6 is similar. With a mesh of  $8 \times 8$  elements, the numerical solution is almost converged for both elements. In contrast, the Q4 element yields less accurate solutions even for a mesh of  $64 \times 64$  elements.

### 13. CONCLUSION

A formulation for the plane 4-node quadrilateral element has been presented. The approach was based on some insight concerning the unmodified isoparametric quadrilateral: The convergence property of that element was traced back to the complete first-order terms of a Taylor series expansions of the element shape functions in the physical co-ordinates. Then additional terms were added to the remaining incomplete higher-order term, all of these being expanded into a second-order Taylor series in the physical co-ordinates. Utilizing the principle of virtual displacements, the element stiffness matrix was obtained in a straightforward procedure.

The proposed element unifies the concept of incompatible modes with the concept of underintegration and stabilization. The formulation exhibits all essential element properties. In particular, numerical solutions of high accuracy are obtained and extensions towards non-linear applications can be made.

Future elaborations of the approach presented may focus on an improvement for the evaluation of element stresses. In the case of a linear elastic material, analytical results for all integrations could be worked out. Furthermore, it may be possible to develop formulations for axisymmetric and 3-dimensional applications. Finally, the concept of Taylor series expansion of element basis functions may be applicable to improve other existing finite elements.

#### ACKNOWLEDGEMENT

This work was sponsored by a Ph.D. grant of the German state of Hessen provided through the Technical University of Darmstadt.

Communications with Prof. Howard L. Schreyer at the University of New Mexico, USA, were particularly helpful to develop conceptual ideas. Important results have been obtained in fruitful collaboration with Prof. B. Daya Reddy at the University of Cape Town, South Africa. Comments provided by Dipl. Math. Michael Imhof at the Technical University of Darmstadt and by Prof. Deborah Sulsky at the University of New Mexico are highly appreciated.

#### REFERENCES

1. I. C. Taig, 'Structural analysis by the matrix displacement method', *English Electric Aviation Limited Report S.O. 17*, 1961.
2. I. C. Taig and R. I. Kerr, 'Some problems in the discrete element representation of aircraft structures', in B. F. Veubeke (ed.), *Matrix Methods of Structural Analysis*, Pergamon Press, Oxford, 1964, pp. 267-315.
3. B. M. Irons, 'Engineering application of numerical integration in stiffness methods', *AIAA J.*, **4**, 2035-2037 (1966).
4. W. P. Doherty, E. L. Wilson and R. L. Taylor, 'Stress analysis of axisymmetric solids utilizing higher-order quadrilateral finite elements', *SESM Report No. 69-3*, Dept. of Civil Eng., University of California, Berkeley, 1969.
5. O. C. Zienkiewicz, R. L. Taylor and J. M. Too, 'Reduced integration technique in general analysis of plates and shells', *Int. j. numer. methods eng.*, **3**, 275-290 (1971).
6. S. F. Pawsey and R. W. Clough, 'Improved numerical integration of thick shell finite elements', *Int. j. numer. methods eng.*, **3**, 575-586 (1971).
7. K. T. Kavanagh and S. W. Key, 'A note on selective and reduced integration techniques in the finite element method', *Int. j. numer. methods eng.*, **4**, 148-151 (1972).
8. D. Kosloff and G. A. Frazier, 'Treatment of hourglass patterns in low order finite element codes', *Int. J. Numer. Anal. Meth. Geomech.*, **2**, 57-72 (1978).
9. D. P. Flanagan and T. Belytschko, 'A uniform strain hexahedron and quadrilateral with orthogonal hourglass control', *Int. j. numer. methods eng.*, **17**, 679-706 (1981).
10. Correction of article by D. P. Flanagan and T. Belytschko, *Int. j. numer. methods eng.*, **19**, 689-710 (1983).
11. T. Belytschko, J. S.-J. Ong, W. K. Liu and J. M. Kennedy, 'Hourglass control in linear and nonlinear problems', *Comput. Methods Appl. Mech. Eng.*, **43**, 251-276 (1984).
12. W. K. Liu and T. Belytschko, 'Efficient linear and nonlinear heat conduction with a quadrilateral element', *Int. j. numer. methods eng.*, **20**, 931-948 (1984).
13. O.-P. Jacquotte and J. T. Oden, 'Analysis of hourglass instabilities and control in underintegrated finite element methods', *Comput. Methods Appl. Mech. Eng.*, **44**, 339-363 (1984).
14. W. K. Liu, J. S.-J. Ong and R. A. Uras, 'Finite element stabilization matrices - a unification approach', *Comput. Methods Appl. Mech. Eng.*, **53**, 13-46 (1985).
15. J. C. Schulz, 'Finite element hourgassing control', *Int. j. numer. methods eng.*, **21**, 1039-1048 (1985).
16. O.-P. Jacquotte, J. T. Oden and E. B. Becker, 'Numerical control of the hourglass instability', *Int. j. numer. methods eng.*, **22**, 219-228 (1986).
17. O.-P. Jacquotte and J. T. Oden, 'An accurate and efficient a posteriori control of hourglass instabilities in underintegrated linear and nonlinear elasticity', *Comput. Methods Appl. Mech. Eng.*, **55**, 105-128 (1986).
18. T. Belytschko and W. E. Bachrach, 'Efficient implementation of quadrilaterals with high coarse-mesh accuracy', *Comput. Methods Appl. Mech. Eng.*, **54**, 279-301 (1986).

19. W. E. Bachrach, W. K. Liu and R. A. Uras, 'A consolidation of various approaches in developing naturally based quadrilaterals', *Comput. Methods Appl. Mech. Eng.*, **55**, 43–62 (1986).
20. T. Belytschko and B. E. Engelmann, 'On flexurally superconvergent four-node quadrilaterals', *Comput. Struct.*, **25**, 909–918 (1987).
21. J. C. Schulz, 'Global mode hourgassing control', *Comput. Methods Appl. Mech. Eng.*, **64**, 553–566 (1987).
22. T. Belytschko and L. P. Bindeman, 'Assumed strain stabilization of the 4-node quadrilateral with 1-point quadrature for nonlinear problems', *Comput. Methods Appl. Mech. Eng.*, **88**, 311–340 (1991).
23. H. L. Schreyer, 'The generation of element stiffness matrices from base matrices in the node space', *Comput. Methods Appl. Mech. Eng.*, **94**, 263–283 (1992).
24. U. Hueck, B. D. Reddy and P. Wriggers, 'On the stabilization of the rectangular 4-node quadrilateral element', *Cerecam Report No. 195*, University of Cape Town, South Africa, March 1993; *Commun. Numer. Methods Eng.*, **10**, 555–563 (1994).
25. R. D. Cook, 'Improved two-dimensional finite element', *ASCE J. Struct. Div.*, **100**, 1851–1863 (1974).
26. R. D. Cook, 'Avoidance of parasitic shear in plane element', *ASCE J. Struct. Div.*, **101**, 1239–1253 (1975).
27. E. L. Wilson, R. L. Taylor, W. P. Doherty and J. Ghaboussi, 'Incompatible displacement models', in S. J. Fenves et al. (eds.), *Numerical and Computer Models in Structural Mechanics*, Academic Press, New York, 1973, pp. 43–57.
28. M. Fröier, L. Nilsson and A. Samuelsson, 'The rectangular plane stress element by Turner, Pian and Wilson', *Int. j. numer. methods eng.*, **8**, 433–437 (1974).
29. M. J. Turner, R. W. Clough, H. C. Martin and L. J. Topp, 'Stiffness and deflection analysis of complex structures', *J. Aeronaut Sci.*, **23**, 805–823, 854 (1956).
30. R. L. Taylor, P. J. Beresford and E. L. Wilson, 'A non-conforming element for stress analysis', *Int. j. numer. methods eng.*, **10**, 1211–1219 (1976).
31. G. Strang and G. J. Fix, *An Analysis of the Finite Element Method*, Prentice-Hall, Englewood Cliffs, N.J., 1973, p. 178.
32. J. C. Simo and M. S. Rifai, 'A class of mixed assumed strain methods and the method of incompatible modes', *Int. j. numer. methods eng.*, **29**, 1595–1638 (1990).
33. J. C. Simo and F. Armero, 'Geometrically non-linear enhanced strain mixed methods and the method of incompatible modes', *Int. j. numer. methods eng.*, **33**, 1413–1449 (1992).
34. T. H. H. Pian, 'Derivation of element stiffness matrices by assumed stress distributions', *AIAA J.*, **2**, 1333–1336 (1964).
35. T. H. H. Pian and K. Sumihara, 'Rational approach for assumed stress finite elements', *Int. j. numer. methods eng.*, **20**, 1685–1695 (1984).
36. J. C. Simo, J. G. Kennedy and R. L. Taylor, 'Complementary mixed finite element formulations for elastoplasticity', *Comput. Methods Appl. Mech. Eng.*, **74**, 177–206 (1989).
37. O. C. Zienkiewicz and R. L. Taylor, *The Finite Element Method*, Vol. 1, 4 edn, McGraw-Hill, London, 1989.
38. Y. K. Cheung and W. Chen, 'Refined hybrid method for plane isoparametric element using an orthogonal approach', *Comput. Struct.*, **42**, 683–694 (1992).
39. K.-Y. Yuan, Y.-S. Huang and T. H. H. Pian, 'New strategy for assumed stresses for 4-node hybrid stress membrane element', *Int. j. numer. methods eng.*, **36**, 1747–1763 (1993).
40. S. Di and E. Ramm, 'On alternative hybrid stress 2D and 3D elements', *Eng. Comput.*, **11**, 49–68 (1994).
41. R. L. Spilker and T. H. H. Pian, 'Hybrid-stress models for elastic-plastic analysis by the initial-stress approach', *Int. j. numer. methods eng.*, **14**, 359–378 (1979).
42. U. Hueck, 'Eine Formulierung für das ebene finite Vier-Knoten-Element', *Dissertation*, Institut für Mechanik, Technische Hochschule Darmstadt, Oktober 1993.
43. J. C. Nagtegaal, D. M. Parks and J. R. Rice, 'On numerically accurate finite element solutions in the fully plastic range', *Comput. Methods Appl. Mech. Eng.*, **4**, 153–177 (1974).
44. T. J. R. Hughes, 'Equivalence of finite elements for nearly incompressible elasticity' *J. Appl. Mech. ASME*, **44**, 181–183 (1977).
45. D. S. Malkus and T. J. R. Hughes, 'Mixed finite element methods—reduced and selective integration techniques: a unification of concepts', *Comput. Methods Appl. Mech. Eng.*, **15**, 63–81 (1978).
46. T. J. R. Hughes, 'Generalization of selective integration procedures to anisotropic and nonlinear media', *Int. j. numer. methods eng.*, **15**, 1413–1418 (1980).
47. J. C. Simo, R. L. Taylor and K. S. Pister, 'Variational and projection methods for the volume constraint in finite deformation elasto-plasticity', *Comput. Methods Appl. Mech. Eng.*, **51**, 177–208 (1985).
48. U. Hueck and H. L. Schreyer, 'The use of orthogonal projections to handle constraints with applications to incompressible four-node quadrilateral elements', *Int. j. numer. methods eng.*, **35**, 1633–1661 (1992).
49. D. J. Allman, 'A quadrilateral finite element including vertex rotations for plane elasticity analysis', *Int. j. numer. methods eng.*, **26**, 717–730 (1988).
50. K. Y. Sze, W. Chen and Y. K. Cheung, 'An efficient quadrilateral plane element with drilling degrees of freedom using orthogonal stress modes', *Comput. Struct.*, **42**, 695–705 (1992).
51. B. Taylor, *Methodus Incrementorum Directa et Inversa*, London, 1715.
52. L. E. Malvern, *Introduction to the Mechanics of a Continuous Medium*, Prentice-Hall, Englewood Cliffs, N.J., 1969.
53. W. L. Hacker and H. L. Schreyer, 'Eigenvalue analysis of compatible and incompatible rectangular four-node quadrilateral elements', *Int. j. numer. methods eng.*, **28**, 687–703 (1989).
54. J. Robinson, 'Some new distortion measures for quadrilaterals', *Finite Elements Anal. Des.*, **3**, 183–197 (1987).

55. E. L. Hoffman, 'Eigensystem analysis of an irregular four-node quadrilateral', *Master's Thesis*, Department of Mechanical Engineering, The University of New Mexico, 1987.
56. K.-Y. Yuan, private communications, June 1993.
57. S. Di, private communications, September 1993.
58. O. C. Zienkiewicz and R. L. Taylor, *The Finite Element Method*, Vol. 2, 4 edn, McGraw-Hill, London, 1991.
59. U. Hueck, H. L. Schreyer and P. Wriggers, 'On the incompressible constraint of the 4-node quadrilateral element', *Int. j. numer. methods eng.*, **38**, 3039–3053 (1995).
60. W. Chen and Y. K. Cheung, 'A new approach for the hybrid element method', *Int. j. numer. methods eng.*, **24**, 1697–1709 (1987).
61. S. P. Timoshenko and J. N. Goodier, *Theory of Elasticity*, 3 edn, McGraw-Hill, New York, 1970, pp. 41–46.
62. T. J. R. Hughes, *The Finite Element Method: Linear Static and Dynamic Finite Element Analysis*, Prentice-Hall, Englewood Cliffs, N.J., 1987.
63. J. C. Simo and T. J. R. Hughes, *Elastoplasticity and Viscoelasticity: Computational Aspects*, Springer, Berlin, in preparation.
64. J. C. Simo and R. L. Taylor, 'Consistent tangent operators for rate-independent elastoplasticity', *Comput. Methods Appl. Mech. Eng.*, **48**, 101–118 (1985).
65. B. D. Reddy and J. C. Simo, 'Stability and convergence of a class of enhanced strain methods', *SIAM J. on Numerical Analysis*, to appear.
66. P. Wriggers and U. Hueck, 'A formulation of the QS6 element for large elastic deformations', *Int. j. numer. methods eng.*, accepted for publication.